SPLICE RESEARCH
Progress Report

UNIFICATION OF FLUSH END-PLATE DESIGN PROCEDURES

by

David M. Hendrick
and
Anant R. Kukreti
Thomas M. Murray
Co-Principal Investigators

Sponsored by

Metal Building Manufacturers Association
and
American Institute of Steel Construction

Report No. FSEL/MBMA 85-01

March 1985

FEARS STRUCTURAL ENGINEERING LABORATORY
School of Civil Engineering and Environmental Science
University of Oklahoma
Norman, Oklahoma 73019

ABSTRACT

This study is on the unification of design procedures for four types of flush end-plate configurations. The four types are: two-bolt unstiffened; four-bolt unstiffened; four-bolt stiffened with a web gusset plate placed between the two rows of tension bolts; and four-bolt stiffened with a web gusset plate placed outside the tension rows of bolts. The resulting end-plate design procedures are based on yield-line analyses and are consistent with regard to philosophy and assumptions among the four connection types. Prediction equations for the bolt forces considering prying action are also developed in a unified manner.

Experimental verification of the end-plate design equations and the bolt force predictions was conducted for all configurations. A comparison among configurations was made based on strength criterion, i.e. required end-plate thickness and resulting connection capacity, and stiffness criterion, i.e. moment capacity for a stiffness limit suitable for rigid framing connections. Based on the experimental results, design methods are recommended using strength criteria and prediction equations for bolt forces. A look at the moment-rotation/beam-line relationship for each configuration was presented as well.

ACKNOWLEDGEMENTS

The research reported here was sponsored by the Metal Building Manufacturing Association and the American Institute of Steel Construction under the guidance of the MBMA Splice Research Subcommittee. Test specimens were provided by Star Manufacturing Company, Mesco Metal Buildings Corporation and Varco-Pruden Buildings AMCA International.

The contents of the paper are the same as the thesis submitted by David M. Hendrick to the faculty of the School of Civil Engineering and Environmental Science, University of Oklahoma, in partial fulfillment of the requirements for the degree of Master of Science.

TABLE OF CONTENTS

LIST OF FIGURES

LIST OF TABLES

UNIFICATION OF FLUSH END-PLATE DESIGN PROCEDURES

CHAPTER I

INTRODUCTION

1.1 Background

Bolted, flush end-plate connections are primarily used as moment-resistant connections in portal frame construction. The popularity of these connections is due to economics, ease of fabrication and the assumption that they provide a rigid moment connection. The flush end-plate is primarily used to connect two beams, referred to as a "splice-plate connection", Figure 1.1(a), but is sometimes used to connect a beam to a column, Figure 1.1(b). Four different types of flush end-plate connection configurations are shown in Figure 1.2. Figures 1.2(a) and (b) show unstiffened flush end-plate configurations with two and four-bolts near the tension flange. Figures 1.2(c) and (d) show stiffened flush end-plate configurations with four bolts near the tension flange. In Figure 1.2(c), a web gusset plate is located on both sides of the web between the two tension rows of bolts, while in Figure 1.1(d) the web gusset plates are located outside the tension rows of bolts. For both configurations, the gusset plates are welded to both the end-plate and the beam web. Throughout the remainder of this report the words web gusset plate and stiffener will be interchanged

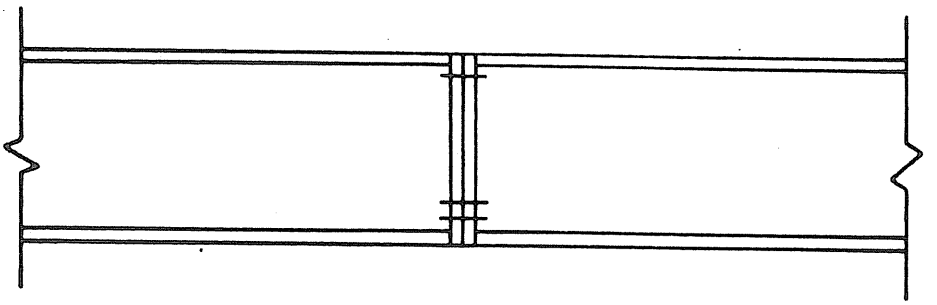

(a) Splice-Plate connection

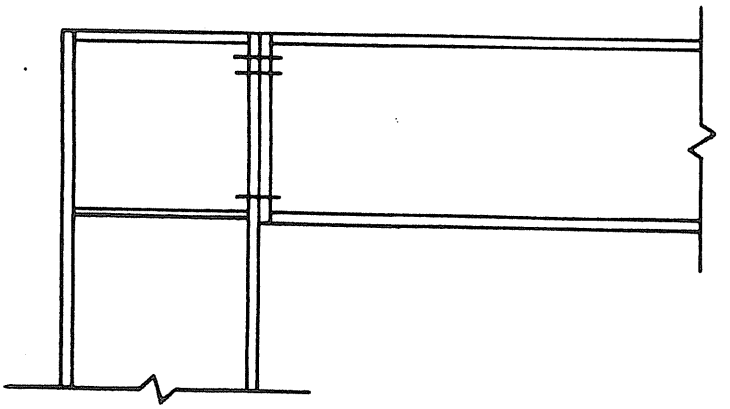

(b) Beam-to-Column Connection

Figure 1.1 Typical Uses of End-Plate Connections

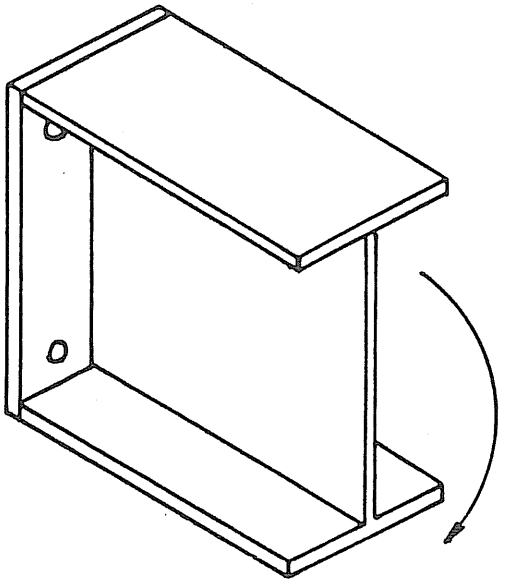

a) Two-Bolt Unstiffened

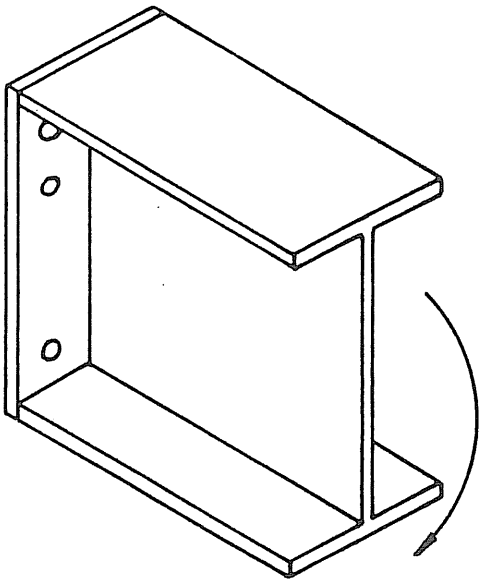

b) Four-Bolt Unstiffened

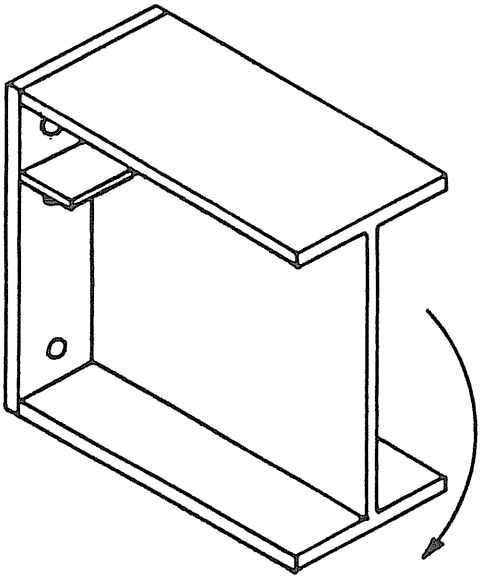

c) Four-Bolt Stiffened with Web Gusset Plate Between the Tension Rows of Bolts

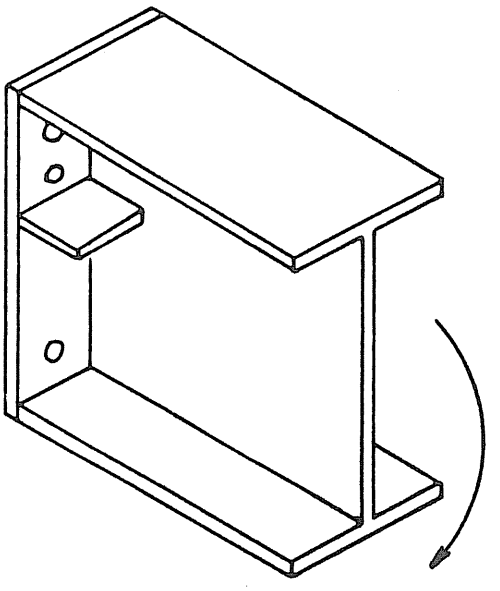

d) Four-Bolt Stiffened with Web Gusset Plate Outside the Tension Rows of Bolts

Figure 1.2 Typical Flush End-Plate Connections

Several design procedures have been suggested to determine end-plate thickness and bolt size based on results from the finite-element method, yield-line theory, or experimental test data. The variation in the resulting thickness for a given loading and configuration has been found to be more than 100% [1]. A much larger variation is found in the prediction of bolt forces since some methods assume that prying action is negligible and does not affect the bolt forces, while other methods require prying action to be considered.

The purpose of this study is to develop a unified set of design equations for end-plate thickness and a corresponding set of prediction equations for bolt forces for the four end-plate connection configurations shown in Figure 1.2. Current literature on the different end-plate design and bolt force prediction procedures is first reviewed followed by the development of yield-line design procedures for the four types of end-plate connections. The end-plate strength design equations are then compared to existing experimental results. In Chapter III the development of bolt force predictions is presented and comparisons to experimental results made. The bolt force equations were developed on the assumption that prying action is of importance and must be considered used in the bolt force calculations. Chapter IV presents a comparison between configurations based on moment-rotation curves and suggested design rules are given for rigid and semi-rigid connections. In Chapter V, the effects of certain geometric parameters are discussed and a design procedure is proposed based on analytical and experimental results. Conclusions and recommendations are then made.

1.2 Literature Review

An extensive review of end-plate connection literature was reported by Srouji et al [1] and will briefly be discussed here. In his review, the design procedures by various authors were presented and end-plate thicknesses were determined based on their recommendations. The principal papers reviewed by Srouji are summarized as follows.

Douty and McGuire [2] in 1965 assumed that extended end-plates cantilever from the top row of the tension bolts under the action of the tension flange forces and a design formula was determined from this assumption. Blockley [3] used a yield-line pattern to calculate flush end-plate thicknesses for two rows of bolts at the tension flange. The beam was assumed to apply the load to the end plate. The German [4] and French Specifications [5] provide equations to find the moment capacity for known plate thicknesses. If the tension bolts are not allowed to exceed the proof load, the equations can be rearranged to determine the end-plate thickness. In 1981, Zoetemeijer [6] presented a theoretical analysis using yield-line theory. The approach was an approximation and hence, necessitated comparison with test results.

Further tests on end-plate connections have been reported by Packer and Morris [7] but limited experimental data did not provide conclusive results. However, Phillips and Packer [8] concluded that flush end-plates with two rows of two bolts near the tension flange are suitable for semi-rigid construction. Kennedy, Vinnakota and Sherbourne [9] used the split tee analogy for certain bolted splices and beam-column connections. Their assumption is that the end-plate goes through three stages of behavior based on

the applied load. The bolt forces are considered to be the sum of a portion of the flange force and prying forces.

Srouji [1] determined the required end-plate thicknesses for a selected set of flush configurations from the methods of the aforementioned authors and found the variation was as large as 100%, see Tables 1.1 and 1.2. Thus, a research program was undertaken by Srouji to study flush end-plate connections. Srouji's work consisted of two and four-bolt unstiffened flush end-plates of the configurations shown in Figure 1.2(a) and (b), respectively, and reported in detail in Reference 1.

The research program was continued by Hendrick et al [10] to include four-bolt stiffened flush end-plates as shown in Figure 1.2(c) and (d). A detailed report on the results of the stiffened flush end-plate study is found in Reference 10. Both studies recommended design procedures using slightly different assumptions concerning bolt force magnitude and prying action force locations. These design procedures are compared and unified in the following chapters.

1.3 Scope of Research

As previously mentioned, the purpose of the research described is to develop design procedures for the four types of end-plates shown in Figure 1.2. The design procedure will provide criteria for:

1. Determination of end-plate thickness using given geometry and material yield stress, e.g., strength criterion.

2. Determination of required bolt diameter including prying effects using given end-plate geometry and thickness, and bolt pretension and proof load forces, e.g.,

Table 1.1

Required Thickness for
Two-Bolt Flush End-Plate Connections

Case No.	Required End-Plate Thickness (in.)					
	Douty & McGuire	German Specification		French Spec.	Zoetemeijer	Kennedy et. al
		Required	Recommended			
F1-3/4-1/2-16	1.27	Ø.71	1.13	1.Ø7	Ø.5Ø	Ø.68
F1-3/4-3/8-16	1.27	Ø.71	1.13	1.Ø7	Ø.5Ø	Ø.49
F1-5/8-1/2-16	1.41	Ø.7Ø	Ø.94	.75	Ø.43	Ø.77
F1-5/8-3/8-16	1.25	Ø.47	Ø.94	.72	Ø.38	Ø.53
F1-5/8-3/8-1Ø	1.17	Ø.38	Ø.94	.7Ø	Ø.36	Ø.54
F1-5/8-1/2-1Ø	1.27	Ø.54	Ø.94	.74	Ø.39	Ø.74
F1-3/4-1/2-24A	1.37	Ø.85	1.13	1.Ø7	Ø.49	Ø.77
F1-3/4-1/2-24B	1.22	Ø.62	1.13	1.Ø4	Ø.46	Ø.73

Notation: F1-3/4-1/2-16 denotes a flush end-plate, one row of 3/4 in. bolts at the tension flange, 1/2" end-plate and a 16 in. depth beam.

Table 1.2

Required Thickness for Four-Bolt Flush End-Plate Connections

Case No.	Douty & McGuire	Blockley	German	French
F2-5/8-1/2-16	1.41	Ø.69	Ø.94	Ø.75
F2-5/8-3/8-16	1.25	Ø.59	Ø.94	Ø.72
F2-3/4-3/8-24	1.37	Ø.78	1.13	1.Ø7
F2-3/4-1/2-24	1.22	Ø.72	1.13	1.Ø4
F2-3/4-1/2-16	1.27	Ø.81	1.13	1.Ø7
F2-3/4-3/8-16	1.27	Ø.81	1.13	1.Ø7

Notation: F2-5/8-1/2-16 denotes a flush end-plate, two rows of 5/8 in. bolts at the tension flange, 1/2 in. end-plate and 16 in. depth beam.

bolt force criterion.

3. Determination of the moment-curvature relationship of the entire connection so that possible effects of connection flexibility can be accounted for in the frame design, e.g., stiffness criterion.

The strength criterion is developed using yield-line analysis for the four types of end-plates from which end-plate thickness is determined. The bolt strength requirements are developed using a modified version of the procedure suggested by Kennedy et al [9]. The stiffness criterion is developed using a beam line concept with moment-rotation curves provided from actual test data.

CHAPTER II

ANALYTICAL STUDY

2.1 Yield-Line Theory

2.1.1 General

Yield-line theory was first introduced to analyze reinforced concrete slabs. A yield-line is a continuous formation of plastic hinges along a straight or curved line. The failure mechanism of the slab is assumed to exist when the yield-lines form a kinematically valid collapse mechanism. Since the elastic deformations are negligible compared to the plastic deformations, it has been proven acceptable to assume that the yield-lines divide the slab into rigid plane regions. Most of the development of this theory is related to reinforced concrete; however, the principles and findings are applicable to steel plates.

Generally, yield-line patterns are assumed to be a series of straight lines; however, some work has been done with curved yield lines. To establish the location of a yield line, the following guidelines must be followed:

1. Axes of rotation generally lie along lines of support.
2. Yield Lines pass through the intersection of the axes of rotation of adjacent plate segments.

3. Along every yield line, the bending moment is assumed to be constant and is taken as the plastic moment of the plate.

The analysis of a yield-line mechanism can be performed by two different methods, the equilibrium method and the virtual work or energy method. The latter method is comparatively simple and straight-forward and is preferred. In this method, the external work done by the applied loads in moving through a small arbitrary virtual deflection field is set equal to the internal work done as the plate rotates at the yield lines to accommodate this virtual deflection field. For a specified yield-line pattern and loading, a certain plastic moment will be required along the hinge lines. For the same loading, other patterns may result in a larger required plastic moment capacity. Hence, the controlling pattern is the one which requires the largest required plastic moment. Or conversely, for a given plastic moment capacity, the controlling mechanism is the one which produces the lowest failure load. This implies that the yield-line theory is an upper bound procedure and the least upper bound must be found.

To determine the required plastic moment capacity or the failure load, an arbitrary succession of possible yield-line mechanisms must be selected. By equating the internal and external work, the relation between the applied loads and the ultimate resisting moments is obtained. The resulting equation is then solved for either the unknown loads or the unknown moments, and by comparing the different values obtained from the various mechanisms the controlling minimum load (or maximum required plastic moment) is obtained.

The internal energy stored in a particular yield-line mechanism is the sum of the internal energy stored in each yield line forming the mechanism. The internal energy stored in any given yield line is obtained by multiplying the normal moment on the yield line with the normal rotation of the yield line. Thus the energy stored, w_{in}, in the n-th yield line of length L_n is

$$W_{in} = \int_{L_n} m_p \, \theta_n \, ds \tag{2.1}$$

where θ_n is the relative rotation of line n, and ds is the elemental length of line n. The internal energy stored, w_{in}, by a yield-line mechanism can be written as

$$\begin{aligned} W_i &= \sum_{n=1}^{N} \int_{L_n} m_p \, \theta_n \, ds \\ &= \sum_{n=1}^{N} m_p \, \theta_n \, L_n \end{aligned} \tag{2.2}$$

where N is the number of yield lines in the mechanism.

For complicated yield-line patterns the expressions for the relative rotation are somewhat tedious to obtain; therefore, it is more convenient to resolve the slopes and moments in the x- and y- directions. This results in the following form of Equation 2.2

$$W_i = \sum_{n=1}^{N} (m_{px} \, \theta_{nx} \, L_x + m_{py} \, \theta_{ny} \, L_y) \tag{2.3}$$

where m_{px} and m_{py} are the x- and y-components of the normal moment capacity per unit length, L_x and L_y are the x- and y-components of the yield line length, and θ_{nx} and θ_{ny}, are the x- and y-components of the relative normal rotation of yield line n.

To calculate the values of θ_{nx} and θ_{ny}, convenient straight lines parallel to the x- and y-axis in the two segments intersecting at the yield-line are selected and their relative rotation calculated by selecting straight lines with known displacements at the end.

2.1.2 Application to Flush End-Plates

A number of yield-line patterns are possible for the flush end-plate geometries defined in Figure 1.2. The controlling yield-line mechanisms used in this study are shown in Figures 2.1 through 2.4. These patterns were determined from a study of possible yield-line patterns and predict the least moment capacity of the sets analyzed.

For all of the end-plates, the external work done due to a unit displacement at the top of the beam flange, resulting in a rotation of the beam cross-section about the outside of the compression flange is given by

$$W_e = M_u \theta \tag{2.4}$$

where M_u = the factored beam moment at the end-plate, and θ = the rotation at the connection, equal to 1/h, where h = beam depth. The internal energy stored in the yield-line mechanism for the two-bolt unstiffened configuration, Figure 2.1, is given by

$$W_i = 4m_p \frac{(h-p_t)}{h} [\ b_f/2(1/p_f+1/s) + (p_f+s)2/g\ ] \tag{2.5}$$

where P_f = the distance from the bolt centerline to the face of the flange, equal to $(P_t - t_f)$, and s = the distance between parallel yield lines, to be determined.

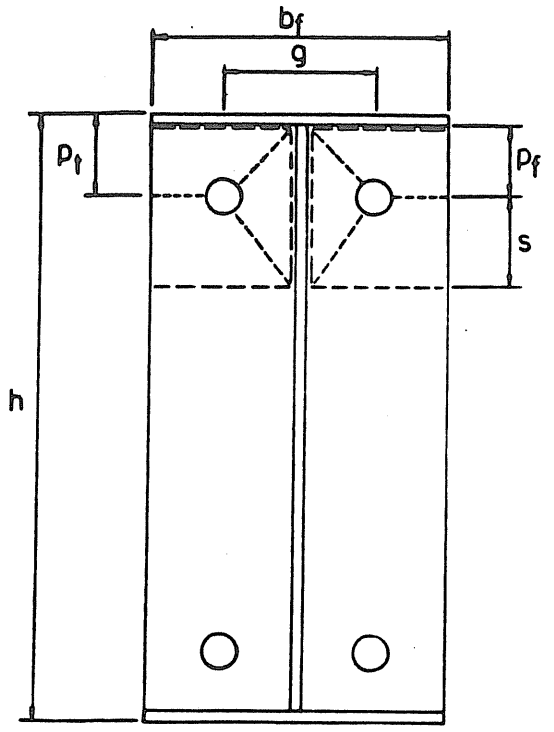

Figure 2.1 Two-Bolt Unstiffened

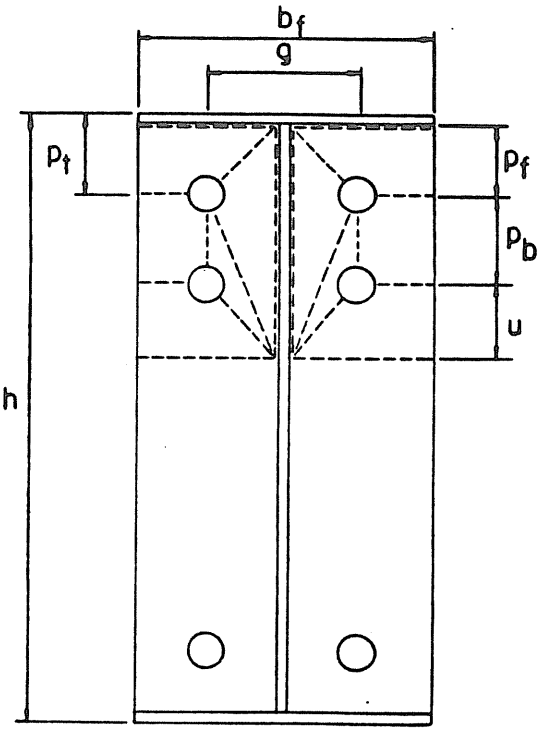

Figure 2.2 Four-Bolt Unstiffened

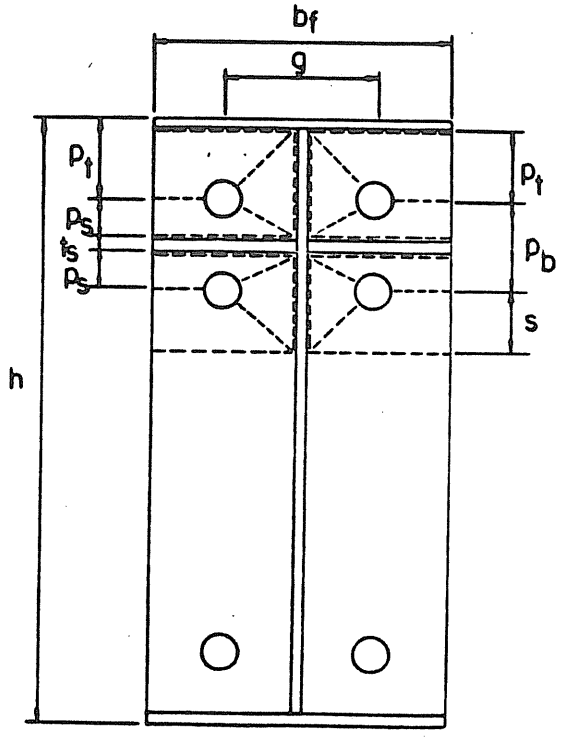

Figure 2.3 Four-Bolt Stiffened Between

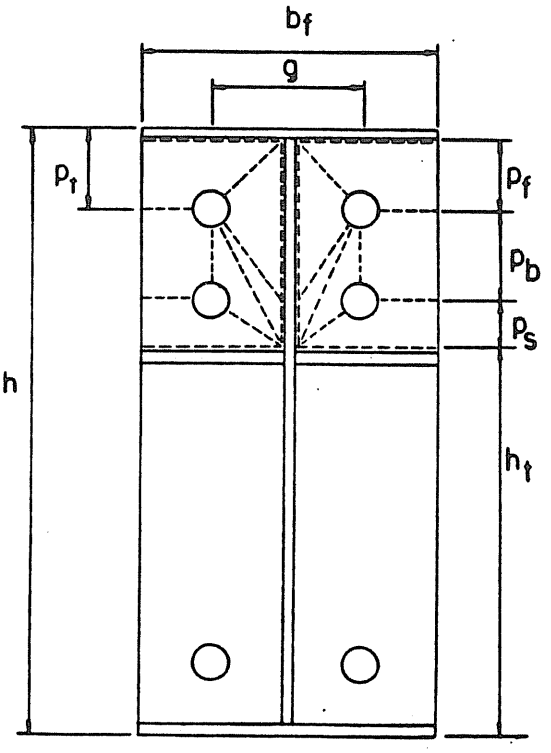

Figure 2.4 Four-Bolt Stiffened Outside

The unknown quantity s in Equation 2.5 is obtained by differentiating the internal work equation with respect to s and equating to zero, resulting in

$$s = 1/2\sqrt{b_f\ g} \tag{2.6}$$

The controlling mechanism for the four-bolt unstiffened configuration is shown in Figure 2.2. The internal energy stored in this mechanism is given by

$$w_i=\frac{4m_p}{h}\left\{(h-p_t)\,[b_f/2\,(1/p_f+1/u)\ +\ 2/g\,(p_f+p_b+u)\,]-b_f p_b/2u\right\} \tag{2.7}$$

where P_b = pitch between bolt rows, and u = the distance between parallel yield lines, to be determined. The unknown quantity u is determined in the same manner as s, e.g., by differentiating the internal work equation with respect to u and equating to zero, resulting in

$$u = 1/2\sqrt{b_f g\ \frac{(h-p_t-p_b)}{(h-p_t)}} \tag{2.8}$$

The internal energy stored in the yield-line mechanism shown in Figure 2.3 for the four-bolt stiffened between the bolt rows configuration is

$$w_i = \Big\{4m_p\ [\ b_f/2\,(1/p_f+1/p_s)\ +\ (p_f+p_s)\,2/g\ ]\ (h-p_t)/h\ +$$
$$[\ b_f/2\,(1/p_s+1/s)\ +\ (p_s+s)\,2/g\ ]\ (h-p_t-p_b)/h\Big\} \tag{2.9}$$

where P_f = the distance from the bolt centerline to the face of the flange, equal to $(p_t - t_f)$, s = the distance between parallel yield lines, equal to equation 2.6, and P_s = distance from the centerline of the bolt to the face of

the stiffener, equal to $1/2(P_b - t_s)$, where t_s = thickness of the stiffener.

The controlling mechanism for the four-bolt flush end-plate with the stiffener outside the bolt rows, Figure 2.4, is very similar to the four-bolt unstiffened flush end-plate. One additional yield-line is formed from the outer bolt toward the web due to an increase in plate separation at the location of the gusset plate. This particular yield-line is based on photographs of the stiffened outside failure mechanisms. A considerable amount of plate separation occurs at the location of the gusset plate when the stiffener is outside the two rows of bolts [10]. If the amount of separation at the stiffener is greater than at the inner row of bolts, then a yield-line would have to form as shown in Figure 2.4 due to two separate slopes coming to one point. If this yield-line did not occur then Figure 2.4 would be identical to Figure 2.2 and no increase in strength would be expected from the stiffened outside configuration. However, from test results the stiffener outside the two rows of bolts increases the strength by approximately 20%. Thus, an additional yield-line must have formed.

The displacement at the gusset plate was assumed to be 25% greater than the displacement along the line of the second row of bolts. The amount of separation at the stiffener was not measured at the time of testing. An assumption of 25% was made and test results for all four stiffened outside tests correlated well with this assumption. The internal energy stored in the mechanism is

$$W_i = 4m_p/h \left\{(h-p_t)[b_f/2p_f + 2/g(p_f+p_b)] + b_f/4 + 1.25(h-p_t-p_b) \times [(1/p_s + 1/2h_t)b_f/2 + g/10p_s + 2/g(p_b/5+p_s)]\right\} \quad (2.10)$$

where h_t = distance from the outer edge of the compression flange to the inner edge of the stiffener, equal to ($h- P_t -P_b-P_s$), and P_s = the distance from the centerline of the inner row of bolts to the inner edge of the stiffener. The additional yield-line formed due to the addition of the stiffener was assumed to form near the web at the centerline of the inner row of bolts. The exact location when assuming a 25% increase in separation would be somewhere between the two rows of bolts and could be found by differentiating the internal work and setting it equal to zero, as previously defined. This was done, but a closed form equation could not be formulated and so it is not possible to find the exact location without performing an iteration using a rather lengthy equation. If the location is assumed at the inner row of bolts, the error in the resulting internal energy is only 1%-2% for practical cases and thus, for design purposes no attempt was made to show the "exact" location of the yield-line.

The yield-line mechanism of Figure 2.4 and the resulting internal energy given by equation 2.10 differs from that suggested by Hendrick in Reference 10. This particular mechanism (Figure 2.4) correlates better with the increase in plate separation at the stiffener and predicts better the actual failure moment of the configuration.

On equating the respective internal and external work terms and cancelling θ, the expression for the ultimate moment, Mu, can be obtained for each configuration. Then by rearranging the expressions for Mu, equations for t_p, the required end-plate thickness, can be written in terms of Mu. The equations for both Mu and t_p for the four types of end-plates follow:

Two-Bolt Unstiffened Flush End-Plate

$$M_u = 4m_p(h-p_t)\ [\ b_f/2(1/p_f+1/s) + (p_f+s)2/g\ ] \quad (2.11)$$

where $m_p = F_{py}Z = F_{py}(t_p^2/4)$

$$t_p = \left\{ \frac{M_u/F_{py}}{(h-p_t)\ [\ b_f/2(1/p_f+1/s) + (p_f+s)2/g\ ]} \right\}^{1/2} \quad (2.12)$$

$p_f = p_t - t_f$ and $s = 1/2\sqrt{b_f g}$

Four-Bolt Unstiffened Flush End-Plate

$$M_u = 4m_p\left\{(h-p_t)[\ b_f/2(1/p_f+1/u) + 2/g(p_f+p_b+u)\ ] - b_f p_b/2u\right\} \quad (2.13)$$

$$t_p = \left\{ \frac{M_u/F_{py}}{(h-p_t)\,[b_f/2(1/p_f+1/u)+2/g(p_f+p_b+u)] - b_f p_b/2u} \right\}^{1/2} \quad (2.14)$$

where $u = 1/2\sqrt{b_f g\ \frac{(h-p_t-p_b)}{(h-p_t)}}$

Four-Bolt Stiffened Flush End-Plate with Gusset Plate Between Tension Bolts

$$M_u = 4m_p\left\{(h-p_t)\ [\ b_f/2(1/p_f+1/p_s) + (p_f+p_s)2/g\ ] + (h-p_t-p_b)\ [\ b_f/2(1/p_s+1/s) + (p_s+s)2/g]\right\} \quad (2.15)$$

$$t_p = \left\{ \frac{M_u/F_{py}}{(h-p_t)\ [\ b_f/2(1/p_f+1/s) + 2/g(p_f+p_s)\ ] + (h-p_t-p_b)\ [\ b_f/2(1/p_s+1/s) + 2/g(p_s+s)\ ]} \right\}^{1/2} \quad (2.16)$$

where $s = 1/2\sqrt{b_f g}$ and $p_s = 1/2(p_b - t_s)$

Four-Bolt Stiffened Flush End-Plates with Gusset Plate Outside Tension Bolts

$$M_u = 4m_p \left\{(h-p_t)\left[b_f/(2p_f) + 2/g(p_f+p_b)\right] + b_f/4 + 1.25(h-p_t-p_b) \times \left[(1/p_s + 1/(2h_t))b_f/2 + g/(10p_s) + 2/g(p_b/5+p_s)\right]\right\} \quad (2.17)$$

$$t_p = \left\{\frac{M_u/F_{py}}{(h-p_t)\left[b_f/(2p_f) + 2/g(p_f+p_b)\right] + b_f/4 + 1.25(h-p_t-p_b) \times \left[(1/p_s + 1/(2h_t))b_f/2 + g/(10p_s) + 2/g(p_b/5+p_s)\right]}\right\}^{1/2} \quad (2.18)$$

where $h_t = h - p_t - p_b - p_s$

In the preceeding equations for four-bolt stiffened and unstiffened end-plates, if p_s is set equal to zero and the stiffener is removed where applicable, the resulting equation will be that for the two-bolt unstiffened flush end-plate. For example, in Equation 2.14 if $p_b = \emptyset$ then u = s and Equation 2.14 becomes identical to Equation 2.12. Likewise, in Equation 2.16 if $p_b = \emptyset$, then the p_s term would not exist since there is not a stiffener in use and Equation 2.16 reduces to Equation 2.12. Similarly, with Equation 2.18, if $P_b = \emptyset$, then p_s and h_t would not exist and Equation 2.18 reduces to Equation 2.12 with one exception. It was assumed that the stiffener outside the bolt rows caused a 25% increase in displacement and an additional yield-line. If the stiffener does not exist than the 1.25 term becomes 1.00 and Equation 2.18 reduces to Equation 2.12.

A similar analysis was performed between the four-bolt

stiffened and unstiffened equations to provide one unified equation for all three four-bolt configurations. However, both stiffened end-plate configurations contain yield-lines that do not exist in the unstiffened configuration. Thus, neither equation will reduce to a form of the other. A unified equation containing variables which would cancel out certain terms depending on which configuration was being used could be developed but would not be appropriate for design purposes. Therefore, no attempt was made to show this unification.

Results from the preceding yield-line analyses are compared to experimental data in the following sections.

2.2 Experimental Verification

To verify the yield-line analytical procedures of Section 2.1, Srouji [1] and Hendrick [10] conducted tests of unstiffened and stiffened flush end-plates, respectively. Srouji's work consisted of eight, two-bolt and six, four-bolt unstiffened tests, while Hendrick tested four, four-bolt end-plates with a gusset plate between the tension rows of bolts and four, four-bolt end-plates with a gusset plate outside the tension rows of bolts. The test setup in both testing programs consisted of end-plates welded to two beam sections and tested as splice connections under pure moment. Figure 2.5 shows the standard test setup for each test. All beam and end-plate material was A572 Gr. 50 steel with A325 bolts used in the connection. The bolts were instrumented on the tension side to monitor bolt strain, and calipers were used at the end-plate connection to measure plate separation. Vertical deflection was also measured at midspan. Bolt pitch, gage and diameter were varied among the test configurations within the limits shown in Table 2.1

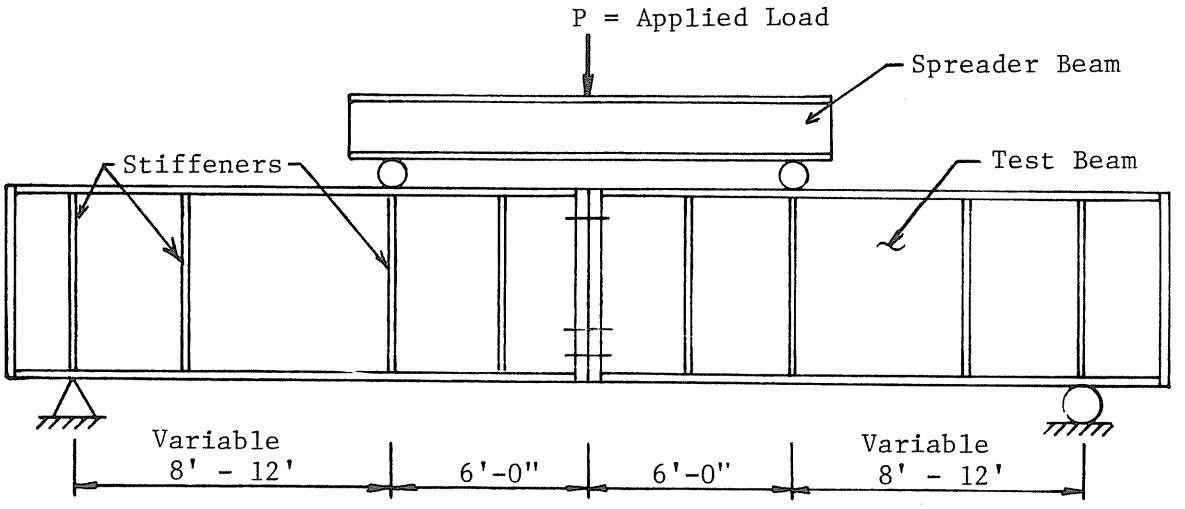

a) Elevation of Test Set-up

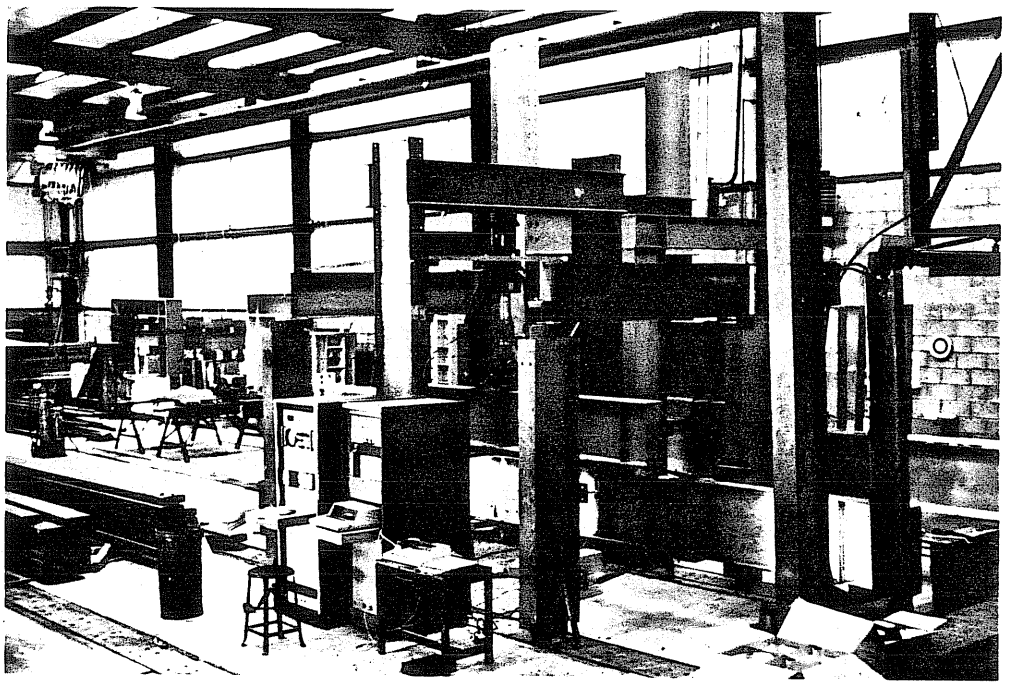

b) Photograph of Test Setup

Figure 2.5 Typical Test Setup

Table 2.1

Limits of Geometric Parameters

Parameter	Low	Intermediate	High
g	2 1/4	2 3/4	3 3/4
d_b	5/8	3/4	1
p_f	1 1/8	1 3/4	2 1/2
p_b	1 7/8	2 3/4	4
b_f	5	7	10
t_p	5/16	1/2	3/4
t_f	.18	.375	.50
t_w	.10	.1875	.375

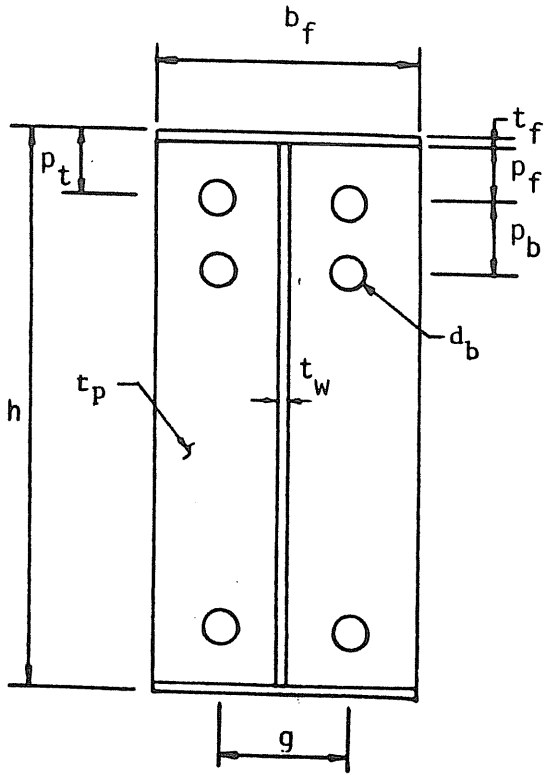

The test specimens were loaded at varying increments to approximately 2/3 of the failure load, unloaded to a load of 2 to 5 kips, and then reloaded until the previous load was increased by 5 to 10%. This procedure was repeated until a yield plateau was reached in either the moment versus centerline deflection or the moment versus plate separation curve or the bolt forces began to greatly exceed the bolt proof load (twice the allowable tension capacity as given in the AISC Manual [13]). The corresponding moment was defined as the failure moment of the end-plate.

Tables 2.2, 2.3, and 2.4 list the nominal geometry of the end-plates for the two-bolt, four-bolt unstiffened, and four-bolt stiffened flush end-plates tested, respectively, and the measured yield stress obtained using coupons cut from identical material. The test designations shown in the tables are to be interpreted as follows: F2-3/4-3/8-16 designates a flush end-plate test with two rows of 3/4 in. diameter bolts at the tension flange. The end-plate thickness is 3/8 in., and the beam depth is 16 in. For one row of bolts, a `1' replaces the `2' in F2. For stiffened flush end-plates, a `B' designates a stiffener was placed between the tension rows of bolts, while an `O' designates a stiffener was placed outside the tension rows of bolts. Tests were conducted using 10 in., 16 in., 23 in., and 24 in. depth beams.

Tables 2.5, 2.6, and 2.7 summarize the strength data for the two-bolt, four-bolt, and four-bolt stiffened flush end-plate tests, respectively. The tables include the maximum applied moment, the predicted failure moment from the previously discussed yield-line mechanisms, and the ratio of maximum applied moment to predicted failure moment. For the two-bolt flush end-plates (Table 2.5) and

Table 2.4

Four Bolt Stiffened Flush End-Plate Test Parameters

Test Designation	Bolt Diameter d_b (in.)	End-Plate Thickness t_p (in.)	Beam Depth h (in.)	Flange Width b_f (in.)	Pitch p_f (in.)	Gage g (in.)	Span Length L (in)	Yield Stress (ksi)
FB2-3/4-3/8-16	3/4	3/8 (.379)	16	6	1 1/2	3 1/2	320	55.48
FO2-3/4-3/8-16	3/4	3/8 (.379)	16	6	1 1/2	3 1/2	330	55.48
FB2-3/4-3/8-24	3/4	3/8 (.366)	24	6	1 3/4	3 1/4	336	52.82
FO2-3/4-3/8-24	3/4	3/8 (.366)	24	6	1 3/4	3 1/4	336	52.82
FB2-5/8-3/8-16	5/8	3/8 (.381)	16	6	1 3/8	2 3/4	321	55.90
FO2-5/8-3/8-16	5/8	3/8 (.381)	16	6	1 3/8	2 3/4	314	55.90
FB2-3/4-1/2-23	3/4	1/2 (.507)	23	6	1 3/4	3 1/4	408	50.07
FO2-3/4-1/2-23	3/4	1/2 (.507)	23	6	1 3/4	3 1/4	408	50.07

Notes: FB2: a 3/8" stiffener was placed between the two rows of tension bolts.
FO2: a 3/8" stiffener was placed outside the two rows of tension bolts.
Flange and web thickness for all tests were 1/4 in. except the 3/4-1/2-23 tests. The flange and web thickness were 3/8 in.
Weld sizes were specified.
(.xxx): Measured thickness.

Table 2.5

Summary of Strength Data
for Two-Bolt Flush End-Plate Tests

Test Number	Actual Failure Moment (ft-k)	Predicted Failure Moment (ft-k)	$\frac{M_{act.}}{M_{pred.}}$	Percent Error
F1-3/4-1/2-16	92.5	90.1	1.03	3%
F1-3/4-3/8-16	54.0	54.3	.99	1%
F1-5/8-1/2-16	77.1	80.0	.96	4%
F1-5/8-3/8-16	64.8	62.0	1.05	5%
F1-5/8-1/2-10	39.5	38.4	1.03	3%
F1-5/8-3/8-10	33.9	31.3	1.08	8%
F1-3/4-1/2-24	154.2	164.5	.94	6%

Table 2.6

Summary of Strength Data for
Four-Bolt Flush End-Plate Tests

Test Number	Actual Failure Moment (ft-k)	Predicted Failure Moment (ft-k)	$\frac{M_{act}}{M_{pred.}}$	Error
F2-5/8-1/2-16	108	109.1	0.99	1%
F2-5/8-3/8-16	85.5	81.6	1.05	5%
F2-3/4-1/2-24	171.8	177.3	0.97	3%
F2-3/4-3/8-24	144.7	136.4	1.06	6%
F2-3/4-1/2-16	115.5	112.2	1.03	3%
F2-3/4-3/8-16	73.2	68.8	1.06	6%

Table 2.7

Summary of Strength Data for
Four-Bolt Stiffened Flush End-Plate Tests

Test Number	Actual Failure Moment (ft-k)	Predicted Failure Moment (ft-k)	$\frac{M_{act}}{M_{pred.}}$	Percent Error
FB2-3/4-3/8-16	95.8	98.1	.98	2%
FO2-3/4-3/8-16	77.4	79.0	.98	2%
FB2-3/4-3/8-24	149.2	141.5	1.05	5%
FO2-3/4-3/8-24	123.2	114.3	1.08	8%
FB2-5/8-3/8-16	111.4	121.5	.92	8%
FO2-5/8-3/8-16	88.0	88.9	.99	1%
FB2-3/4-1/2-23	257.0	243.3	1.06	6%
FO2-3/4-1/2-23	210.0	198.6	1.06	6%

the yield-line mechanism of Figure 2.1, the ratio of maximum applied moment to predicted failure moment varied from Ø.94 to 1.Ø8. For the four-bolt flush end-plate (Table 2.6) and the mechanism of Figure 2.2, the ratio varied from Ø.97 to 1.Ø6. Finally, for the four-bolt stiffened flush end-plates (Table 2.7) and the mechanisms of Figures 2.3 and 2.4, the ratio of maximum applied moment to the predicted failure moment varied from Ø.92 to 1.Ø8, respectively.

Thus, the test results from the twenty-one flush end-plate tests conducted by Srouji and Hendrick show that the yield-line mechanisms of Figures 2.1 through 2.4 and the corresponding strength equations, Eq. 2.11 through 2.18, adequately predict the failure moment for the two-bolt, four-bolt, and four-bolt stiffened flush end-plate configurations if the geometric parameters are within the limits of Table 2.1. The ratio of maximum applied moment to predicted failure moment for all tests was between Ø.92 and 1.Ø8. The average value was 1.Ø2 with a standard deviation of Ø.Ø5.

A comparison among configurations tested cannot directly be made because of the difference in geometric parameters of each individual test. However, since the yield-line analyses predict the failure moment within $\pm$8%, a comparison of predicted failure moments can be made. For comparison purposes, the geometric parameters of the four-bolt, unstiffened flush end-plate tests of Table 2.2 were chosen. For a two-bolt connection, P_b is taken as zero. For the stiffened between connections, the stiffener is placed halfway between the two rows of bolts, and for the stiffened outside connections, the stiffener is placed at a distance of one bolt diameter plus one-half inch from the inner row of bolts. For all tests, the yield stress is

Table 2.8

Comparison of Predicted Flush End-Plate Strength Data

Test	Predicted Failure Moment (ft-kips)				Ratio					
			Four-Bolt Stiffened							
	Two Bolt (1)	Four Bolt (2)	Between (3)	Outside (4)	(2)/(1)	(3)/(1)	(4)/(1)	(3)/(2)	(4)/(2)	(3)/(4)
FX-5/8-1/2-16	81.6	102.4	157.5	131.7	1.25	1.93	1.61	1.54	1.29	1.20
FX-5/8-3/8-16	56.9	74.0	104.9	90.1	1.30	1.85	1.58	1.42	1.22	1.17
FX-3/4-1/2-24	138.9	180.1	274.8	224.3	1.30	1.98	1.62	1.52	1.24	1.23
FX-3/4-3/8-24	88.5	117.0	170.0	141.5	1.32	1.92	1.60	1.45	1.21	1.20
FX-3/4-3/8-16	50.3	63.4	95.1	76.7	1.26	1.89	1.53	1.50	1.21	1.24
FX-3/4-1/2-16	89.4	112.6	169.1	136.4	1.26	1.89	1.53	1.50	1.21	1.24
Average					1.28	1.91	1.58	1.49	1.23	1.21
Standard Deviation					0.03	0.04	0.04	0.04	0.03	0.03

Table 2.9

Summary of Strength Data for Flush End-Plates

Two-Bolt	Four-Bolt		
	Unstiffened	Stiffened Between	Stiffened Outside
1.0	1.3	1.9	1.6
	1.0	1.5	1.2
		1.0	0.8

55 ksi. Analytical results for the six configurations are found in Table 2.8.

The ratio of the predicted failure moment of the four-bolt unstiffened connections to that of the two-bolt connections was found to vary from 1.25 to 1.32. If a stiffener is placed between the two bolt rows, the ratio increases to between 1.85 and 1.98. If the stiffener is placed outside the bolt rows, the corresponding ratio varies from 1.53 to 1.62.

Comparisons between the four-bolt stiffened and unstiffened flush end-plates shows that by placing a stiffener between the bolt rows, the ratio of strengths varies from 1.42 to 1.54. If the stiffener is outside the bolt rows, the strength ratio varies between 1.21 and 1.29. Finally, in comparing only the stiffened end-plates, the predicted strength is 17 to 24% greater if the stiffener is between the bolt rows rather than outside the bolt rows.

In conclusion, Table 2.9 provides a summary of two-bolt and four-bolt stiffened and unstiffened flush end-plate strength data ratios. The four-bolt, stiffened between configuration is 90% stronger than a two-bolt configuration, 50% stronger than a four-bolt unstiffened configuration, and 20% stronger than a four-bolt stiffened outside configuration. The four-bolt, stiffened outside configuration is 60% stronger than a two-bolt configuratiion and 20% stronger than a four-bolt unstiffened configuration. Likewise, the four-bolt unstiffened configuration is 30% stronger than the two-bolt configuration.

The preceeding yield-line mechanisms and corresponding test results were limited to specified geometric

parameters. Significant changes in the geometric relationships could affect the mechanism configuration and thus, the predicted capacity. The following limitations apply to the end-plate design equations presented herein:

$$p_f \leq 2.0 \quad , \qquad t_p/d_b \leq 1.0 \ ,$$

$$g \leq 4.0 \quad , \text{ and } \quad b_f/g \leq 2.25 \ .$$

CHAPTER III

BOLT FORCE PREDICTIONS

3.1 Estimation of Bolt Forces

Basic yield-line analysis procedures do not result in bolt forces if prying action is to be considered. Therefore, it was necessary to find a different method to obtain the desired bolt forces. A method suggested by Kennedy et al[9] was modified to estimate bolt forces due to both applied force and prying action. The basis of the method is the split-tee analogy and three stages of end-plate behavior are defined. During the first stage, which occurs under low applied loads, the end-plate is referred to as "thick" since no plastic hinges have developed. The upper limit of this behavior, the "thick plate limit", occurs at a load which first causes yielding in the end-plate at the beam flange. Once this load is exceeded, a plastic hinge forms at the beam flange and the end-plate is of "intermediate" thickness and is in its second stage of behavior. As the load is further increased, a second plastic hinge forms at the bolt lines, and the end-plate is considered to be a "thin" plate. The Kennedy split-tee analytical model for bolt forces is shown in Figure 3.1.

Kennedy et al consider the bolt force to be the sum of a portion of the flange force and prying forces. The amount of prying action corresponds to the stage of

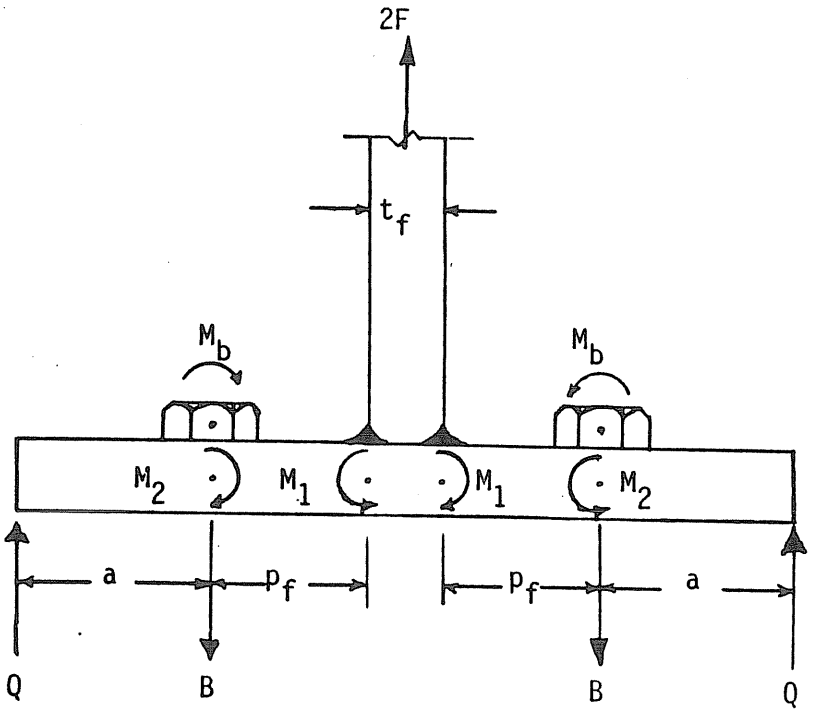

Figure 3.1 Kennedy et. al. Analytical Model

behavior the end-plate is within. When the end-plate is "thick" the amount of prying action is negligible and is taken as zero. When the end-plate is "thin" the prying force is at its maximum value. For "intermediate" behavior, the prying force is somewhere between zero and its maximum value. The equation for the maximum prying force is given as

$$Q_{max} = \frac{w' t_p^2}{4a} \sqrt{F_{py}^2 - 3\left(\frac{F'}{w' t_p^2}\right)^2} \qquad (3.1)$$

where Q_{max} = maximum prying force, w' = width of end-plate per bolt at a bolt line minus the bolt hole, t_p = end-plate thickness, a = distance from edge of end-plate to bolt line, F_{py} = yield stress of the end-plate, and F' = flange force per bolt. The limiting value for the location of the prying action,"a", has been suggested by Mann and Norris [11] to be a = 2.5 d_b and by Nair et al [12] to be a $\leq$ 2tp. Kennedy has suggested that "a" be between $2d_b$ and $3d_b$ as an initial trial value. For "intermediate" end-plates, the equation for prying force is given as

$$Q = \frac{Fp_f}{a} - \frac{b_f t_p^2}{8a} \sqrt{F_{py}^2 - 3\left(\frac{2F}{b_f t_p^2}\right)^2} - \frac{\pi d_b^3 F_{yb}}{32a} \qquad (3.2)$$

The analytical model of Figure 3.1 was modified by Srouji [1] as shown in Figure 3.2 for the two-bolt, flush end-plate and as shown in Figure 3.3 for the four-bolt, flush end-plate. The two-bolt model is essentially one-half of the original analytical model. The force in each bolt is one-half of the flange force plus prying action forces. The four-bolt model is similar to the two-bolt model with the addition of a second row of bolts. The force in the second row of bolts is also unknown which produces an indeterminate problem. In order to obtain the

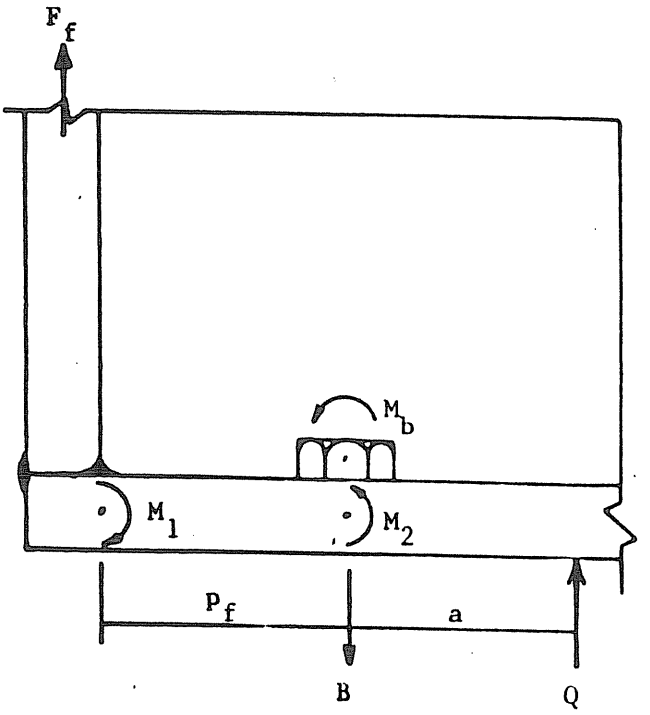

Figure 3.2 Modified Kennedy Model for Two-Bolt Flush End-Plate

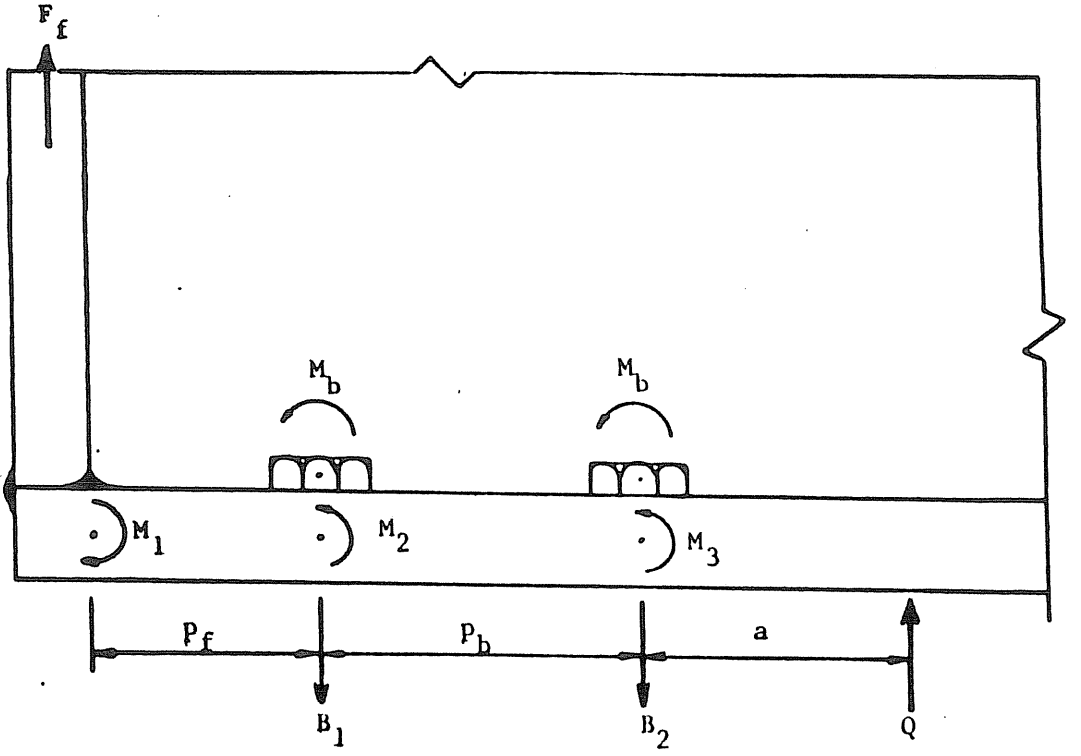

Figure 3.3 Modified Kennedy Model for Four-Bolt Flush End-Plate

bolt forces for this particular model, assumptions had to be made concerning the force in the inner row of bolts. The force in the inner bolt, B_2, was assumed to be a function of the flange force, F_f, depending on the stage of end-plate behavior. Srouji assumed that for "thick" end-plates, B_2 is zero, for "intermediate" end-plates, $B_2 = F_f/10$, and for "thin" end-plates, $B_2 = F_f/6$. These values were determined from experimental results. The force in the outer bolt was then taken as the remaining flange force plus the force due to prying.

A second assumption made by Srouji was in the location of the prying action, the "a" distance. In the split-tee analogy of Figure 3.1, the value of "a" was limited between $2d_b$ and $3d_b$ because of a definite distance to the edge of the end-plate. However, for flush end-plates, the location of prying action is below the bolt line and is not limited to the edge of the end-plate. Srouji suggested using $a = t_p$ if $t_p/d_b < 2/3$ and $a = 2t_p$, otherwise. The resulting bolt force predictions and experimental data for the two and four-bolt flush end-plates tested by Srouji are presented in Reference 1. Hendrick used the same assumptions with the four-bolt stiffened flush end-plate configurations and his bolt force predictions and experimental results are presented in Reference 10.

To unify design procedures for the four end-plate configurations considered in this study, modifications were made in the previous assumptions concerning "a" and B_2. First, the assumption of a constant "a" distance if t_p/d_b is greater than or less than 2/3 was not found to correlate well with actual test data or logic. If t_p is increased with all other parameters held constant, the prying force will increase by Equation 3.1. This contradicts the theory that a thicker end-plate would have a smaller prying force

than a thin end-plate. Thus, the location of the prying action was modified to be a function of t_p/d_b. To better approximate the location of the prying action force, values for "a" were assumed and the resulting bolt force predictions were compared to experimental data. Figure 3.4 shows the variation of "a" (from the best predicted/experimental fit for each of the twenty-one tests) versus t_p/d_b. As seen in Figure 3.4, as the ratio t_p/d_b increases, the "a" distance also increases. By fitting the best curve to the test data points, an empirical equation for the location of prying action was found to be

$$a = 3.682\ (t_p/d_b)^3 - 0.085 \qquad (3.3)$$

The second modification concerns the assumption for the inner row bolt force. Since the location of the prying action was modified by Equation 3.3, the assumption $B_2 = F_f/6$ for "thin" end-plates was found not to correlate as well. To improve the predicted/experimental correlation for four-bolt unstiffened and stiffened outside configurations, B_2 is taken equal to $F_f/8$. When the stiffener is placed between the bolt rows, the inner bolt force will increase due to a part of the flange force being transferred to the stiffener and B_2 is taken as $F_f/5$. It is again noted that these assumptions are based on experimental data and found by curve fitting the predicted and experimental data. For "thick" and "intermediate" end plates, Srouji's assumptions were found to be adequate for all four configurations, that is, $B_2 = 0$ and $B_2 = F_f/10$, respectively.

Using all of the above, the following steps are to be used to predict bolt forces including prying action for two- and four-bolt, stiffened or unstiffened, flush moment

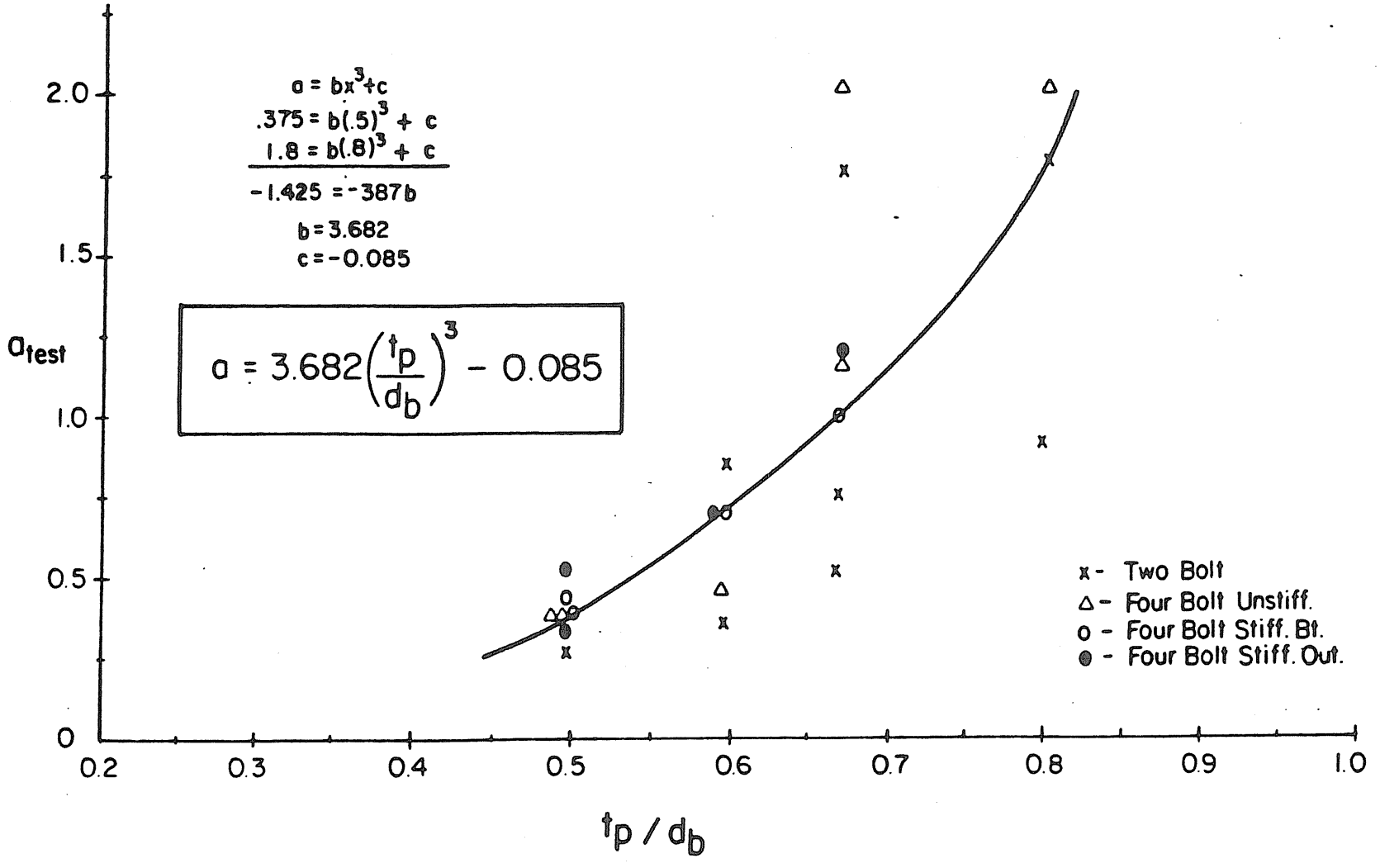

Figure 3.4 Empirical Derivation Plot for Prying Force Location

end-plate connections.

1. With a given end- plate moment for which the bolt forces are to be determined, calculate the resulting flange force, F_f,

$$F_f = M/(d-t_f) \tag{3.4}$$

2. Find the thick plate limit, t_1, using the following approximate equation

$$t_1 = \sqrt{4.21\ P_f F_f/(b_f F_{py})} \tag{3.5}$$

Then refine the value using the following exact iterative equation:

$$t_1 = \sqrt{\frac{4 p_f F_f}{b_f \sqrt{F_{py}^2 - 3\left(\frac{F_f}{b_f t_1}\right)^2}}} \tag{3.6}$$

Once the thick plate limit is determined, the actual end-plate thickness, t_p, is compared to it. If $t_p > t_1$, then the prying force, Q is taken as Ø, otherwise, Q = Ø and the next step is used.

3. Find the thin plate limit, t_{11}, using the following approximate equation

$$t_{11} = \sqrt{\frac{2(F_f p_f - \pi\ d_b^3 F_{yb}/16)}{F_{py}(Ø.85 b_f/2 + Ø.8 w')}} \tag{3.7}$$

where F_{yb} = yield stress of the bolt. Then refine the value using the exact iterative equation:

$$t_{11} = \sqrt{\frac{2(F_f p_f - \pi d_b^3 F_{yb}/16)}{\frac{b_f}{2}\sqrt{F_{py}^2 - 3\left(\frac{F_f}{b_f t_{11}}\right)^2} + w'\sqrt{F_{py}^2 - 3\left(\frac{F_f}{2w' t_{11}}\right)^2}}} \qquad (3.8)$$

When performing the iterations in the thin-plate stage, if the flange force becomes large, i.e., greater than the beam capacity, a negative value could occur under the radical in equation 3.8. If this occurs then the end-plate is failing due to shear effects rather than yielding due to bending. Thus, the following limitation should always be satisfied before performing iterations with Equation 3.8:

$$F_f < 2w' t_{11} F_{py} / \sqrt{3} \qquad (3.9)$$

where t_{11} is found from Equation 3.7. If Equation 3.9 is not satisfied, the beam capacity must be increased so that shear failure does not occur. Again the end-plate thickness is compared to t_{11}. If $t_p > t_{11}$, the plate is intermediate and one of two equations for prying action is used. Equation 3.2 is used to determine the prying force for one-row, two-bolt, flush end-plate connections, which is repeated below

$$Q = \frac{F p_f}{a} - \frac{b_f t_p^2}{8a}\sqrt{F_{py}^2 - 3\left(\frac{2F}{b_f t_p^2}\right)^2} - \frac{\pi d_b^3 F_{yb}}{32a} \qquad (3.2)$$

where F = flange force per bolt = $F_f/2$ and "a" is found from Equation 3.3. The following is used for the two-row, four-bolt flush end-plate connections:

$$Q = \frac{F_2(p_f + 0.1 p_b)}{(a+p_b)} - \frac{b_f t_p^2}{8(a+p_b)}\sqrt{F_{py}^2 - 3\left(\frac{2F_2}{b_f t_p^2}\right)^2} - \frac{\pi d_b^3 F_{yb}}{16(a+p_b)}$$

(3.10)

where $F_2 = F_f/2$ and p_b = pitch between bolt rows.

The bolt force, B, for two-bolt, flush end-plate connections is equal to

$$B = F_f/2 + Q \tag{3.11}$$

but B must be greater than the pretension force. The outer bolt force in the four-bolt, flush end-plate connections is given by

$$B_1 = F_f/2.5 + Q \tag{3.12}$$

where B_1 = the outer row bolt force. Again, B_1 must be greater than the pretension force.

4. If $t_p < t_{11}$ the end-plate is said to be thin and the prying force is at its maximum. From equation 3.1, which is repeated below:

$$Q_{max} = \frac{w' t_p^2}{4a}\sqrt{F_{py}^2 - 3\left(\frac{F'}{w' t_p}\right)^2} \tag{3.1}$$

where F' is the lesser of the following:

$$F_{limit} = \frac{t_p^2 F_{py}(\emptyset.85 b_f/2 + \emptyset.80 w') + \pi d_b^3 F_{yb}/8}{4 p_f} \tag{3.13}$$

or $F_{max} = (F_f)_{max}/2$

The bolt force for two-bolt, flush end-plate connections is then given by

$$B = F_f/2 + Q_{max} \tag{3.14}$$

For four-bolt, stiffened outside and unstiffened, flush end-plate connections, the outer bolt force is then given by

$$B_1 = 3F_f/8 + Q_{max} \qquad (3.15)$$

If a stiffener is placed between the two rows of tension bolts, the outer bolt force is given by

$$B_1 = 3F_f/10 + Q_{max} \qquad (3.16)$$

Bolt forces that are calculated using the above procedure are compared to experimentally obtained forces in the following section.

3.2 Experimental Verification of Bolt Forces

To verify the modified Kennedy method for determining bolt forces, instrumented bolts were used in the tests conducted by Srouji and Hendrick. The bolts were installed at the tension side of the connection after calibration. Reported bolt forces were calculated from strain data assuming elastic material properties and a modulas of elasticity of 29,000 ksi.

Figure 3.5 shows typical plots of bolt force versus moment for the four different end-plate configurations. Appendix B contains the bolt force versus moment plots for each of the twenty-one end-plate tests.

The measured bolt forces were close to values predicted using the previously discussed assumptions and procedures to near the bolt proof load (twice the allowable tension capacity given in the AISC Manual [13]). The corresponding moment at proof load is designated as M_{yb} and

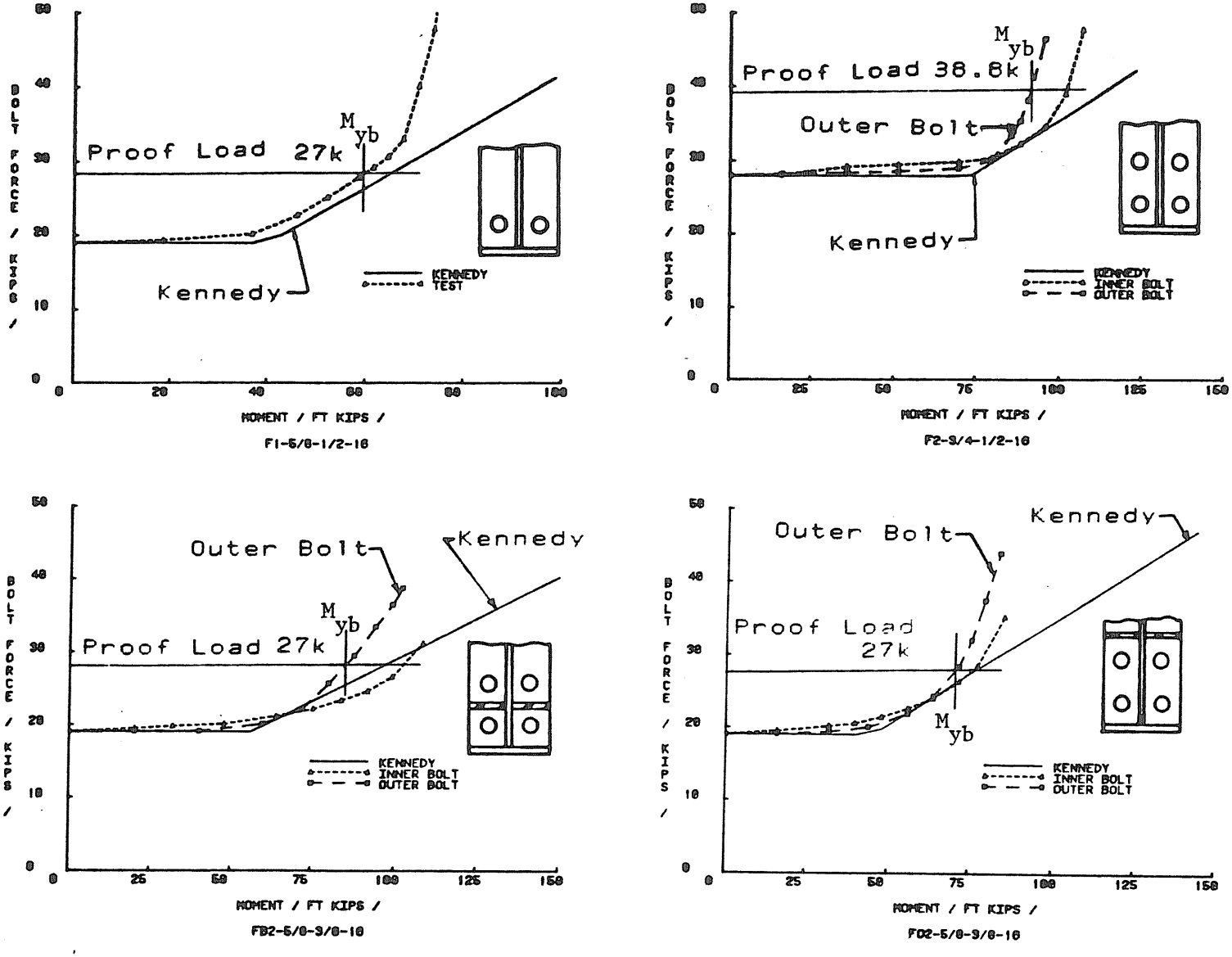

Figure 3.5 Typical Bolt Force Versus Moment Relationship

is shown on each figure in Appendix B and listed in Table 3.1. For all tests, the bolt forces remained near the pretension load up to approximately 50% of the failure moment. At these levels the bolt forces began to increase gradually with increase in applied load and then rapidly as prying action reached its maximum force and excessive plate separation began to occur.

From Appendix B, the two-bolt predictions were slightly unconservative, (10% to 20%), for a majority of the tests, but adequate for design purposes. The four-bolt unstiffened bolt force predictions were in good agreement, (5% to 10%), with the experimental data. For this configuration, the inner and outer bolt forces remained approximately equal until the end-plate reached the "thin" plate stage at which point the outer bolt began to increase more rapidly. Results for Test F2-5/8-3/8-16, Appendix B, are poor due to premature failure of the end-plate which caused increased plate separation and larger bolt forces. The measured four-bolt stiffened end-plate bolt forces are in excellent agreement, (0% to 5%), with the modified Kennedy predictions. Like the four-bolt unstiffened tests, the inner and outer bolt forces remained approximately equal until prying action and plate separation began to occur. The outer bolt forces then increased to 110% to 120% of the inner bolt forces.

Table 3.1 presents ratios of bolt proof load moment, M_{yb}, to the maximum applied moment for all tests. The ratios for the two-bolt tests ranged from 0.62 to 0.99, for the four-bolt unstiffened tests from 0.63 to 1.10, and for the four-bolt stiffened tests from 0.75 to 1.10. Also listed in Table 3.1 are the ratios of the thick plate limit moment, M_{th}, to the maximum applied moment. These ratios varied from 0.52 to 0.86 for the two-bolt tests, 0.47 to

Table 3.1

Bolt Force Yield Moment Comparisons

Test Designation	Failure Moment M_u	M_{th} (ft-k)	M_{yb} (ft-k)	M_{th}/M_u (ft-k)	M_{yb}/M_u
F1-3/4-1/2-16	92.5	59	64*	Ø.64	Ø.69
F1-3/4-3/8-16	54.Ø	46	54	Ø.85	1.ØØ
F1-5/8-1/2-16	77.1	4Ø	48	Ø.52	Ø.62
F1-5/8-3/8-16	64.8	34	58	Ø.52	Ø.9Ø
F1-5/8-1/2-1Ø	39.5	22	25	Ø.56	Ø.63
F1-5/8-3/8-1Ø	33.9	28	29	Ø.83	Ø.86
F1-3/4-1/2-24	154.2	89	137	Ø.58	Ø.89
F2-5/8-1/2-16	1Ø8.Ø	51	68	Ø.47	Ø.63
F2-5/8-3/8-16	85.5	45	39	Ø.53	Ø.46
F2-3/4-1/2-24	121.8	116	18Ø*	Ø.68	1.Ø5
F2-3/4-3/8-24	144.7	84	136	Ø.58	Ø.94
F2-3/4-1/2-16	115.5	77	92	Ø.67	Ø.8Ø
F2-3/4-3/8-16	73.2	59	73	Ø.81	Ø.81
FB2-3/4-3/8-16	95.8	74	1Ø4*	Ø.77	1.Ø9
FO2-3/4-3/8-16	77.4	6Ø	8Ø	Ø.78	1.Ø3
FB2-3/4-3/8-24	149.2	113	161	Ø.76	1.Ø8
FO2-3/4-3/8-24	123.2	87	135	Ø.71	1.1Ø
FB2-5/8-3/8-16	111.4	6Ø	83	Ø.54	Ø.75
FO2-5/8-3/8-16	88.Ø	44	69	Ø.5Ø	Ø.78
FB2-3/4-1/2-23	257.Ø	15Ø	183	Ø.58	Ø.71
FO2-3/4-1/2-23	21Ø.Ø	114	171	Ø.54	Ø.81

* Extrapolated

M_{th} = "thick" plate moment by modified Kennedy method

M_{yb} = moment at which the experimental bolt force is at the proof load (twice the allowable) of the bolt.

Ø.8Ø for the four-bolt unstiffened tests, and Ø.5Ø to Ø.78 for the four-bolt stiffened tests. Very little difference was found between tests with the stiffener between or outside the bolt rows.

For design purposes, the end-plate should be "thick" under service loads, "intermediate" under factored loads, and function as a "thin" plate at ultimate loads. From the experimental results, the end-plate acts as a "thick" plate up to 5Ø-6Ø% of the maximum applied load. The bolt forces reached proof load at approximately 8Ø-9Ø% of the maximum applied load.

CHAPTER IV

MOMENT-ROTATION RELATIONSHIPS

4.1 Types of Connections

The rotational stiffness and moment resistance of connections can be represented using a moment-rotation (M-Ø) diagram as shown in Figure 4.1. This type of diagram is generally obtained through experimental data. The slope of the curve provides an indication of the stiffness of the connection. A steeper slope represents a stiffer connection. Figure 4.2 shows M-Ø curves for typical rigid (Type I), semi-rigid (Type III), and simple (Type II) connections. An "ideal" rigid connection would be a vertical line along the ordinate representing zero rotation. An "ideal" simple connection would follow the abscissa denoting zero moment capacity.

To determine the end moment generated by the connection, a beam line can be constructed on the M-Ø diagram, as shown in Figure 4.3. The beam-line intersects the moment or vertical axis at the beam's fixed end moment $wL^2/12$, and intersects the rotation or horizontal axis at the simple span rotation of the beam. The intersection of the moment-rotation (M-Ø) curve and the beam line gives the rotation of the connection for a particular moment.

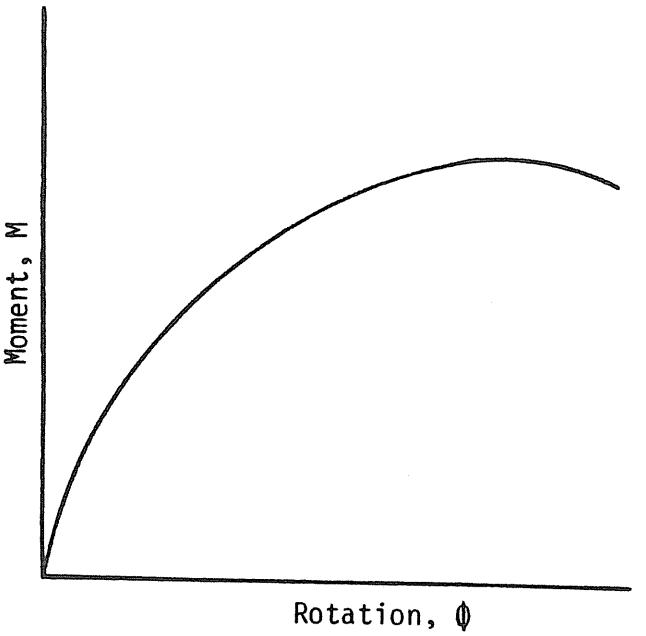

Figure 4.1 Typical Moment-Rotation Diagram

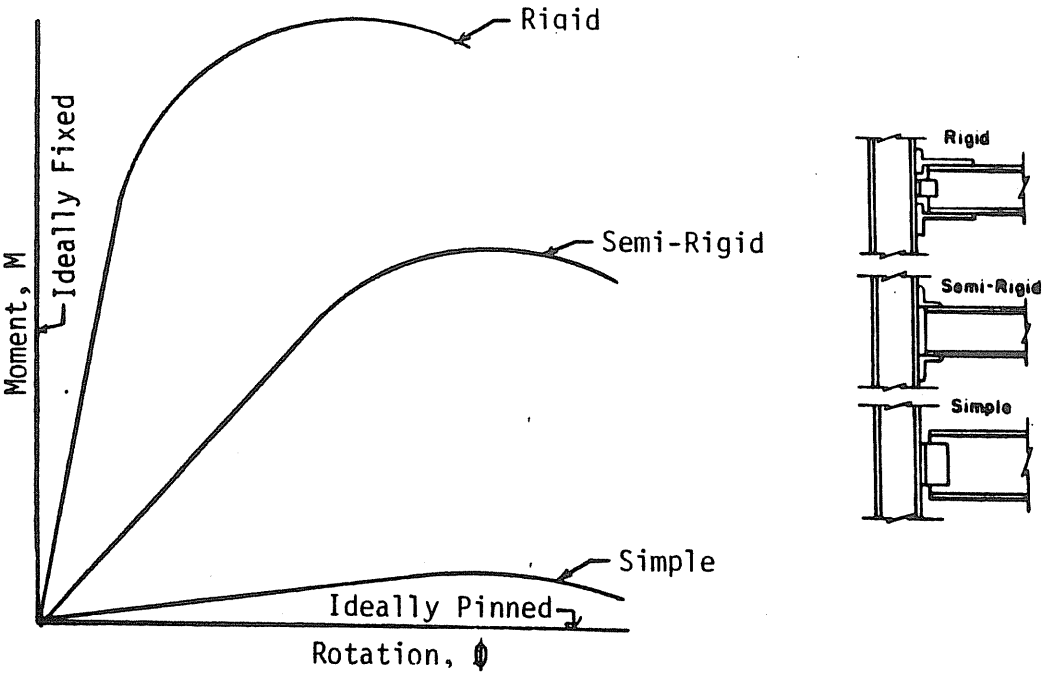

Figure 4.2 Classification of Typical Connections

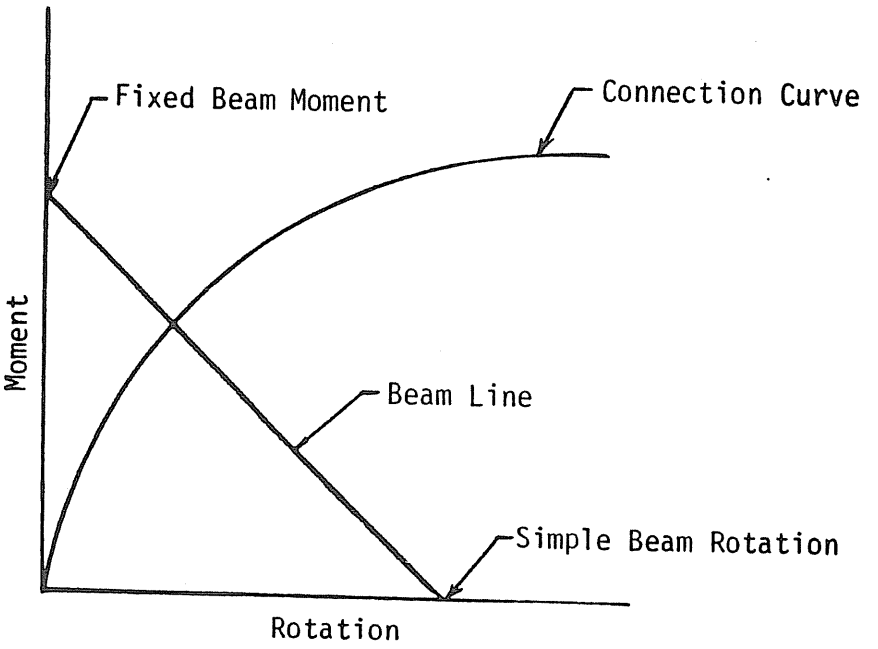

Figure 4.3 Moment-Rotation Relationship

The AISC Specification[13] recognizes three types of construction for design of splice-plate and beam-column connections. Type I or "rigid-frame" construction assumes that the connections have sufficient rigidity to resist rotation at the joints and is unconditionally permitted by the Specification. Type II or "simple framing" construction assumes that the connnections are free to rotate under gravity loads and are connected for shear only, provided there is adequate capacity to resist wind moments, and the girders can carry the full gravity load as "simple beams". Type III or "semi-rigid framing" assumes that the connection has a known and dependable moment capacity intermediate between a "rigid" and a "simple" connection.

4.2 Experimental Results

Typical plots of moment versus rotation (M-Ø) for the two and four-bolt flush end plates tested by Srouji and Hendrick are shown in Figure 4.4. A plot of moment versus rotation and corresponding beam-line for each test is given in Appendix C. The rotation of the connection, Ø, was determined by solving

$$\Delta exp = \Delta theor + ØL/2 \qquad (4.1)$$

for Ø. In this equation, Δ_{exp} is the experimental centerline deflection of the connection at load P, Δ_{theor} is the centerline theoretical deflection at the same load P, and L is the total span length. The connection behaves as a Type I connection up to a certain percentage of the failure moment of the end-plate at which point the curve begins to soften and falls into the Type III connection area. The moment at which the connection reaches 1Ø% of its simple support rotation is defined here to be the

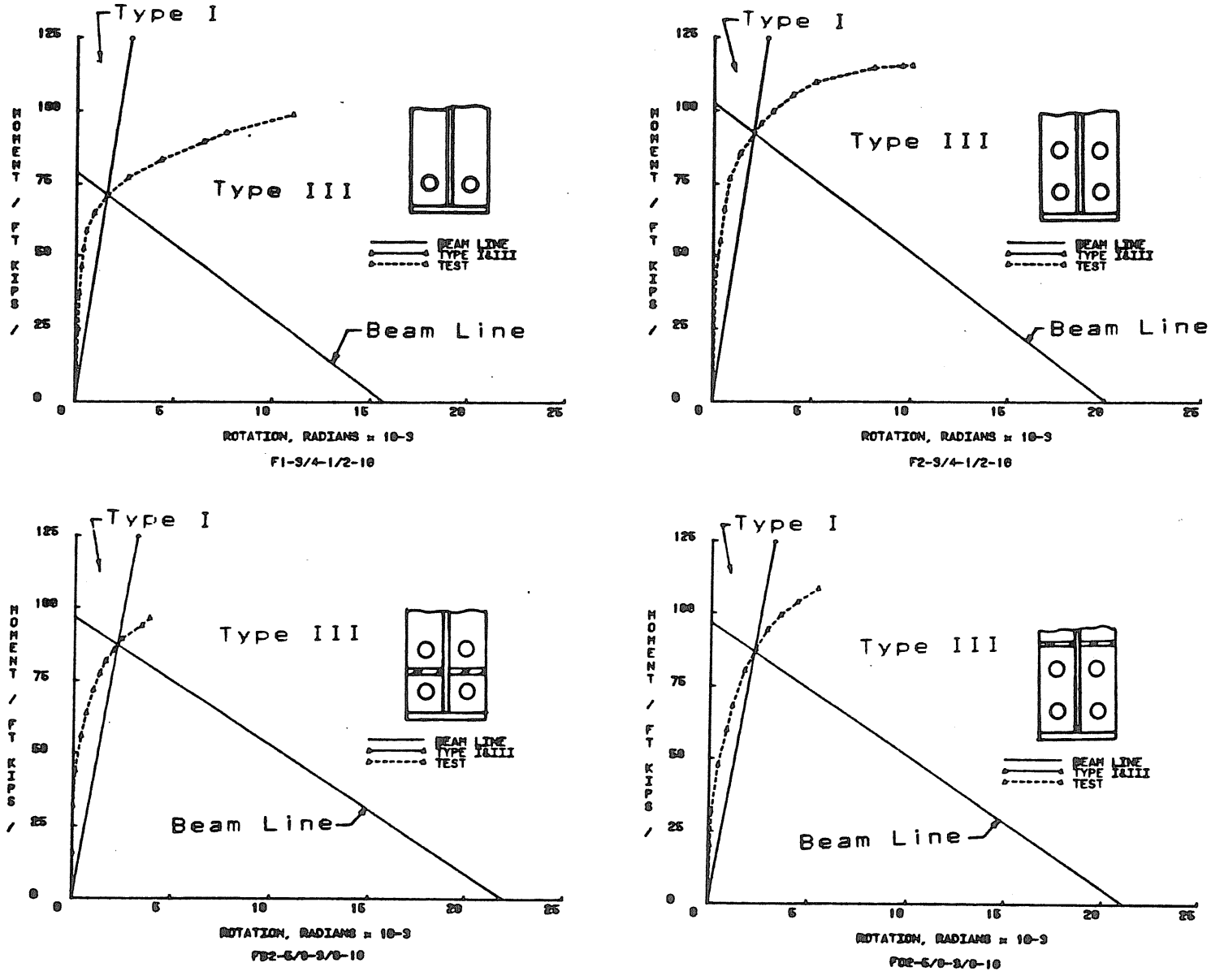

Figure 4.4 Moment vs Rotation Relationship

limiting moment between Type I and Type III connections. Shown in Figure 4.4 is the beam-line based on the test beam length, , the dividing line between a Type I and Type III connection, and the actual rotation of the connection from experimental data for one test of each configuration. Similar plots for all tests are found in Appendix C.

For each connection and M-Ø curve, an infinite number of beam lines can be constructed. First, a fixed-end moment is assumed and the corresponding load is found. The simple support rotation due to that load is then computed. At 1Ø% of this rotation, the Type I and Type III dividing moment can be found. The beam lines shown in Figure 4.4 were found by an iterative process of assuming a number of fixed end moments and comparing the 1Ø% rotations with actual test data. The moment at which the 1Ø% rotation equals the test rotation is the dividing moment between the Type I and Type III connection.

The beam line constructed on the moment-rotation curves depends on the assumed fixed-end moment, M_f, and the corresponding simple support rotation, $\phi=M_f(L/2EI)$. Thus, the beam line is a function of the total span length, L, the modulas of elasticity of the material, E, and the moment of inertia of the section, I. The beam lines shown in Figure 4.4 and in Appendix C were based solely on the specific span length used for each test. By varying the span length and keeping the section capacity constant, the slope of the beam line will vary. Figure 4.5 depicts this change in beam line slope. The connection curve shown is from Test F2-3/4-1/2-16. As seen in the figure, as the span length increases the moment for which the connection is suitable for Type I connection increases. As the length decreases, the limiting moment for a Type I connection will decrease. For this particular connection and a length of

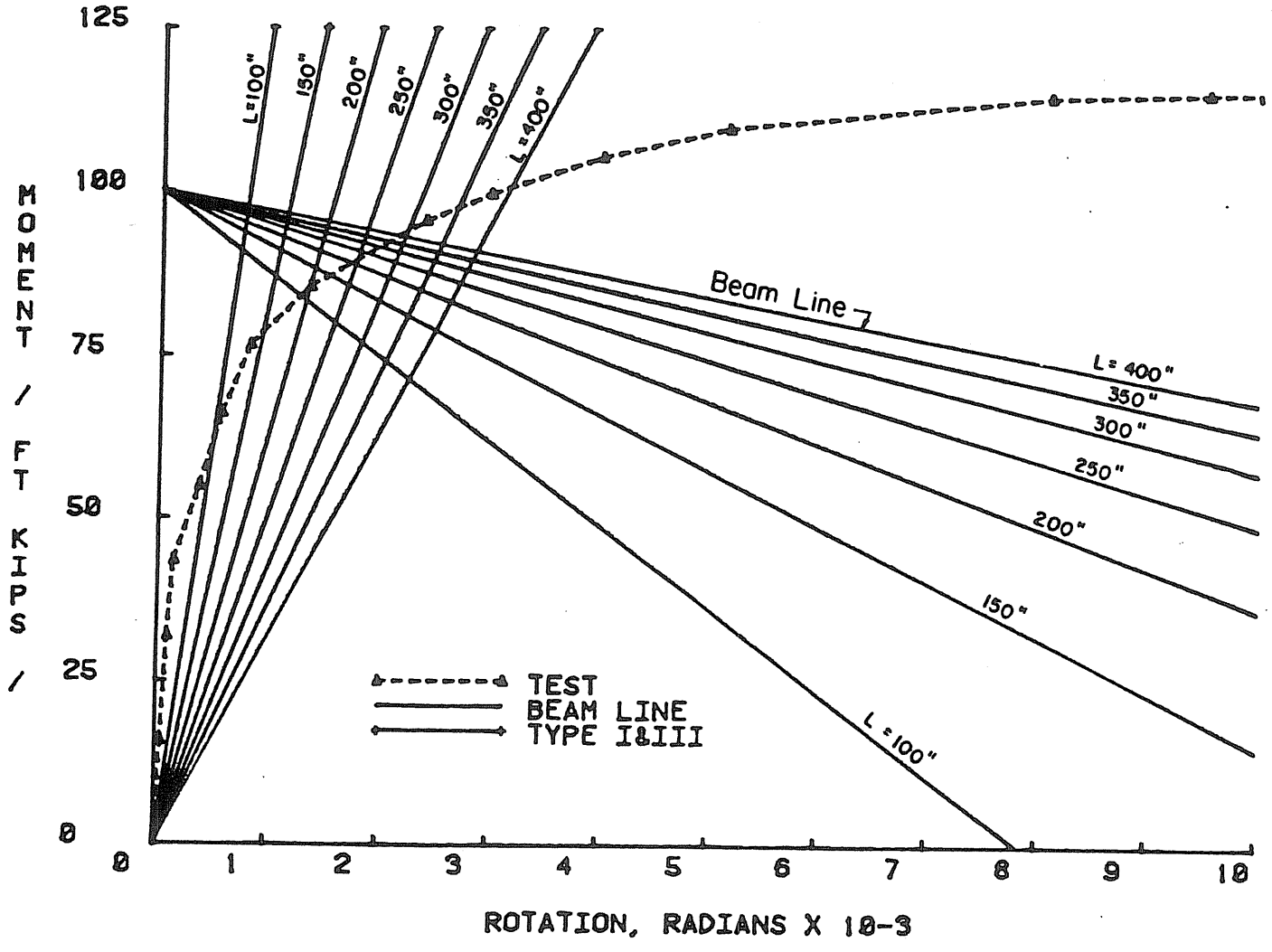

Figure 4.5 Moment Versus Rotation Relationship with Varying Span Length

100 in., the limiting moment for a Type I connection is 63 ft-kips or 54% of the failure moment. If the length is increased to 400 in. the limiting moment is 100 ft-kips or 86% of the failure moment. Because the variation in length causes an increase or decrease in the Type I limiting moment, a general design recommendation for each configuration based on stiffness cannot be made.

It is again emphasized that the moment-rotation curves shown in Figure 4.4 and Appendix C are based on the actual length of the test setup. Using these lengths, the limiting moment for Type I Construction for a two-bolt, flush end-plate varies from 61% to 85% of the failure moment of the connection with an average of 77% and a standard deviation of 8%. For a four-bolt, unstiffened, flush end-plate, the Type I range is 73% to 98% of the failure moment with an average of 88% and a standard deviation of 11%. The range for Type I connection with four-bolt, stiffened, flush end-plates is 63% to 104% when the stiffener is between the tension rows of bolts and 74 to 99% when the stiffener is outside the tension rows of bolts. The average for the stiffened between and stiffened outside connections is 85% and 87%, respectively, with standard deviations of 18% and 10%, respectively,. For all flush end-plate configurations tested , the average limiting moment for a Type I connection using the span length of each test setup is 83% of the failure moment with a standard deviation of 12%.

4.3 Comparisons Among Configurations

A direct comparison of moment-rotation curves among configurations cannot be made because only one set of tests had identical geometric parameters for all four end-plate configurations, and the results were inconclusive.

However, a comparison can be made with the limiting moment for a Type I Construction connection for each end-plate configuration. Figure 4.6 shows for each flush end-plate configuration the dispersion of the ratio of the limiting moment for Type I Construction to the failure moment of the connection. The limiting moment is defined as the intersection of the beam-line and the connection curve using the span length from each individual test. As seen from the figure, the four-bolt stiffened and unstiffened end-plates have approximately equal stiffness, with Type I average limiting moment ratios between Ø.85 and Ø.88. The two-bolt connection has a Type I average limiting ratio of Ø.77. Thus, the four-bolt flush, end-plate connections are approximately 1Ø%-14% stiffer than the two-bolt flush, end-plate connection.

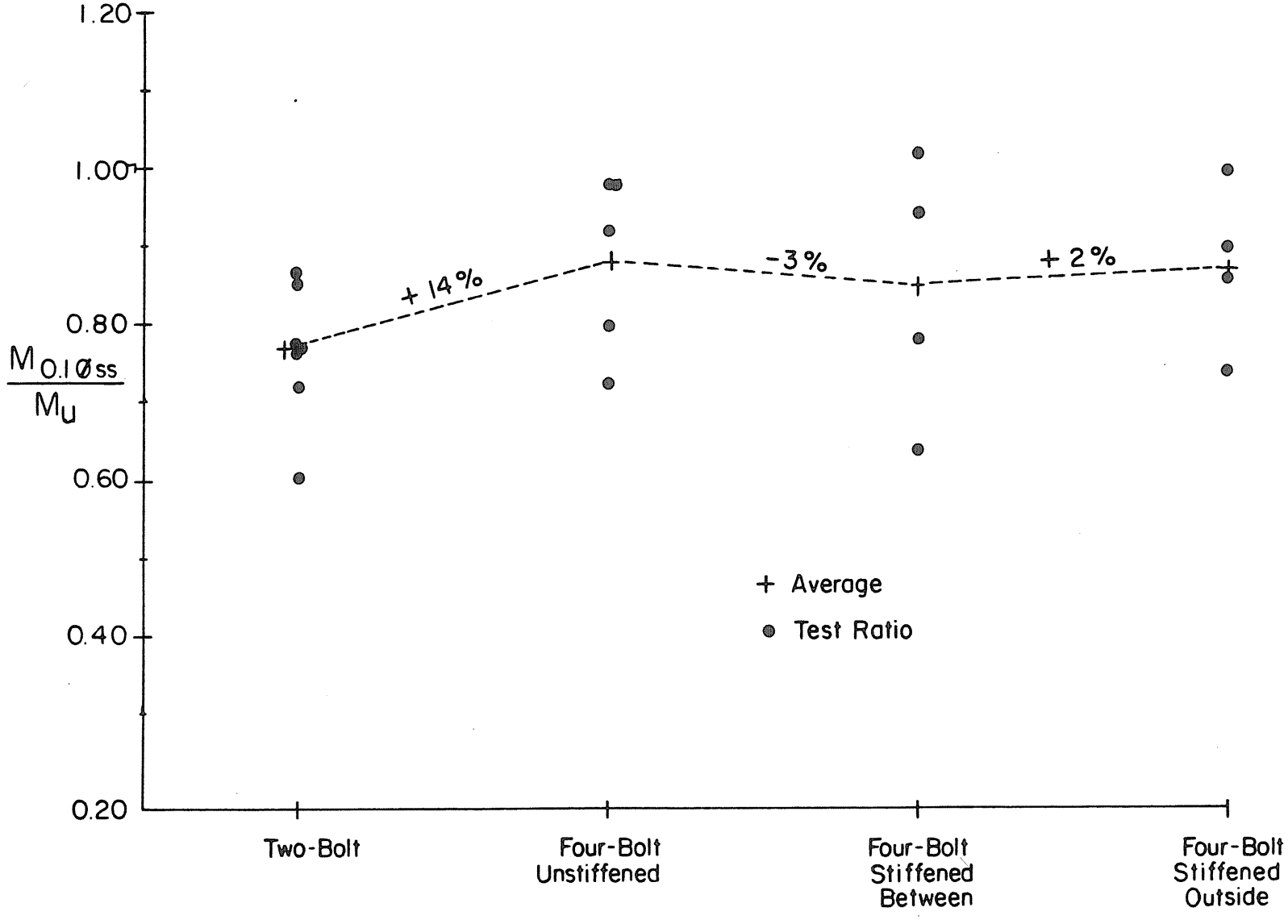

Figure 4.6 Moment-Rotation Comparison

CHAPTER V

DESIGN OF FLUSH END-PLATES

5.1 Effect of Parameters on End-Plate Thickness

Several parameters have effects on the end-plate thickness required from the aforementioned yield-line mechanism equations. The most important parameters were found to be the gage, g, and the bolt pitch, p_f, to the outer row of bolts. The width of the end-plate and the depth of the beam also affect the magnitude of the required thickness. In order to determine relative effects, a four-bolt, unstiffened end-plate connection with the following basic parameters was used: b_f = 8 in., t_f = Ø.375 in., p_f = 1.75 in., p_b = 3/4 in., d_b = 3/4 in., h = 24 in., t_w = Ø.375 in., and F_y = 55 ksi. The quantities g, p_t, b_f, and h were varied individually along with the applied moment to determine effects on end-plate thickness. The results are plotted in Figures 5.1 through 5.4.

Figure 5.1 shows the variation of required end-plate thickness with changes in bolt gage. The required plate thickness was found to increase with increasing gage. For a given moment, at smaller gages the rate of increase in end-plate thickness with increase in gage is slightly larger than at larger gages. However, end-plate thickness is relatively unaffected by change in gage.

Figure 5.2 shows the variation of required plate

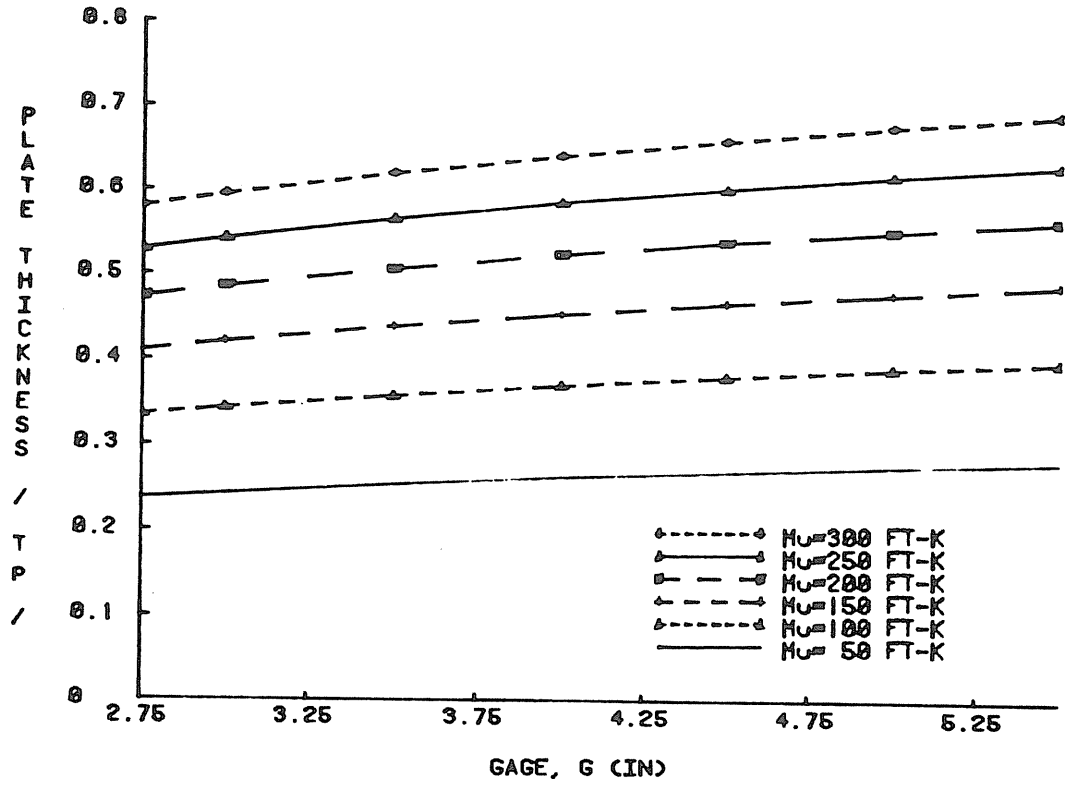

Figure 5.1 Variation of End-Plate Thickness with Gage

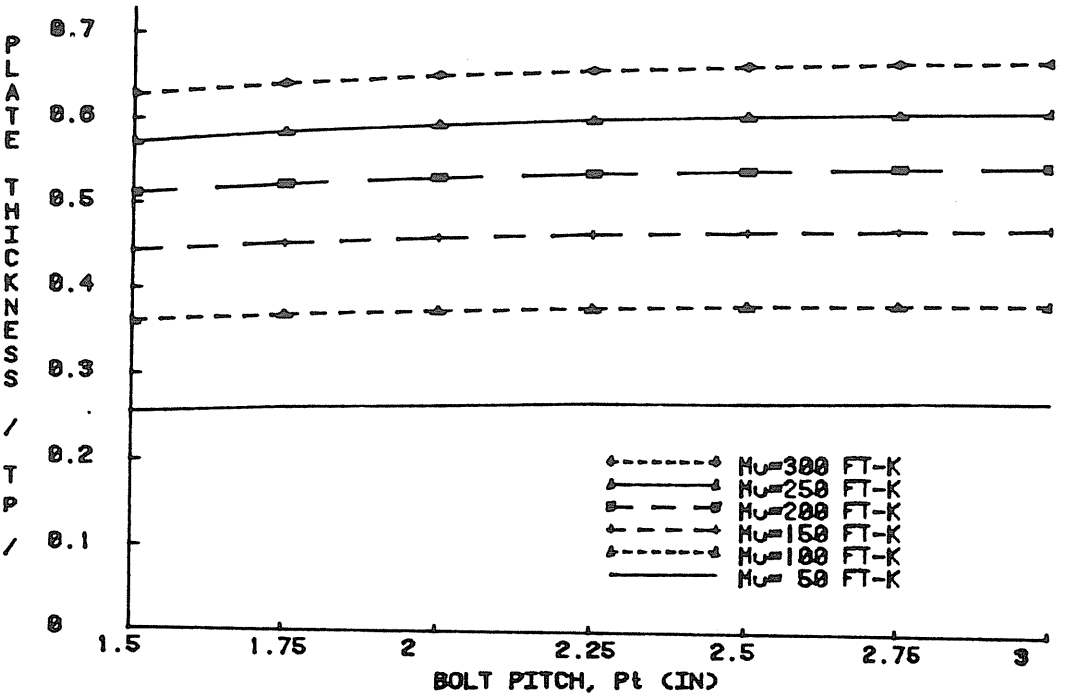

Figure 5.2 Variation of End-Plate Thickness with Bolt Pitch

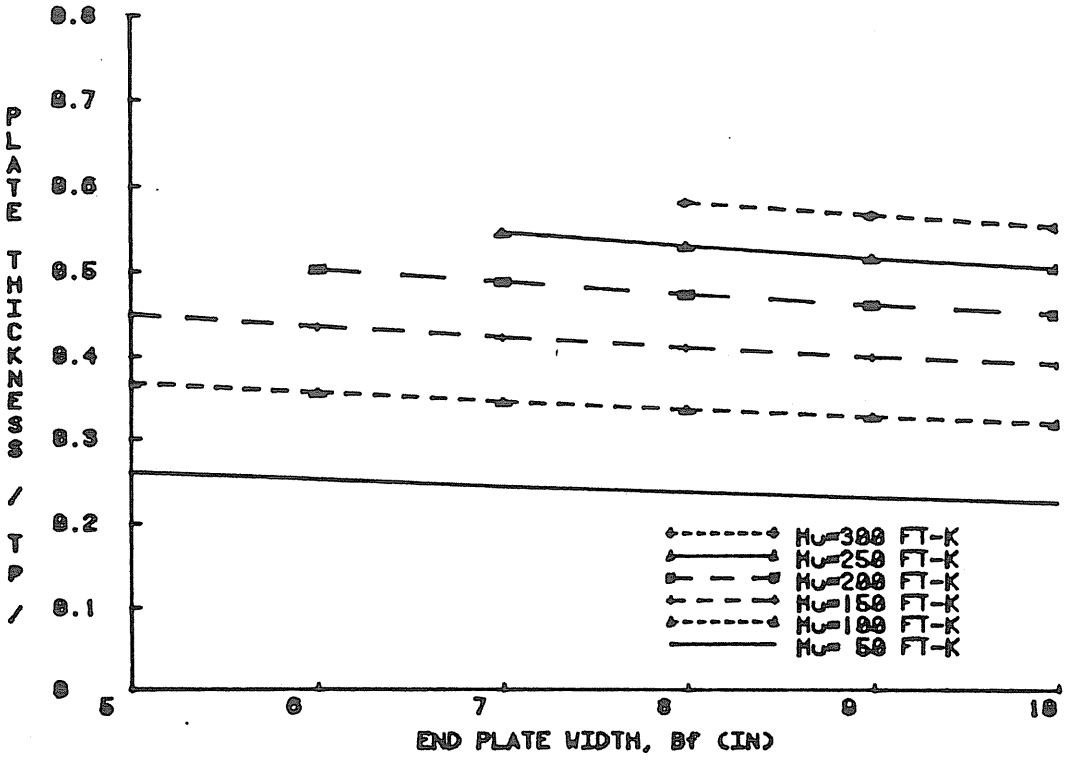

Figure 5.3 Variation of Moment and End Plate Width

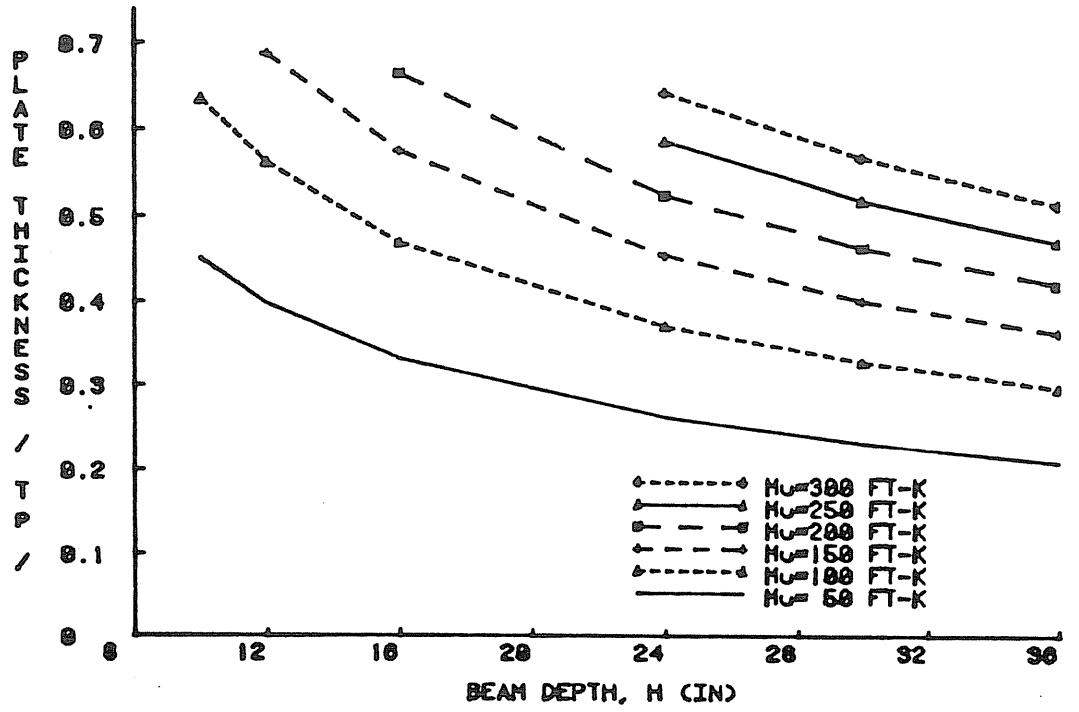

Figure 5.4 Variation of Moment and Beam Depth

thickness with changes in bolt pitch. The results are very similar to what was found for variation in gage; as the bolt pitch increases the required plate thickness also increases. Also, at lower pitches the rate of increase is slightly higher. Again, end-plate thickness is relatively unaffected by change in pitch.

Figure 5.3 shows the variation of required end-plate thickness with changes in end-plate width. As the end-plate width increases, the required plate thickness decreases slightly. Only reasonable end-plate thicknesses were considered to develop the data shown in Figure 5.3.

Figure 5.4 shows the variation of required end-plate thickness with changes in beam depth. For a given moment, as the beam depth is increased the required plate thickness decreases. As the beam depth gets large, i.e., greater than 24 in., the decrease in plate thickness is not as substantial. However, a substantial change is seen when increasing from a 12 or 16 in. depth to a 24 in. depth.

One other parameter, the pitch between bolts, p_b, for four-bolt connections can also affect the required plate thickness. Increasing the pitch between bolt rows decreases the required plate thickness of unstiffened and stiffened outside connections but increases the plate thickness of stiffened between connections. However, as p_b is increased, the bolt forces will also increase so no benefit is obtained. A pitch between the minimum p_b and approximately four bolt diameters is recommended.

5.2 Design Recommendations

For the two-bolt, four-bolt, and four-bolt stiffened flush end-plates with the range of geometries used in this

research, it is recommended that Equations 2.12, 2.14, 2.16, and 2.18, respectively, be used to determine end-plate thickness for a given ultimate design moment. For stiffness requirements, the limiting moment for Type I Construction, as mentioned in Section 4.2, is a function of the span length. A design recommendation for any span cannot be made unless an equation for the connection curve is developed to represent a variation in span length. For the design examples to follow, the span length will be assumed to be the length used in each experimental test and the following guidelines for Type I & Type III Construction can be used for the specific span lengths used in the testing program:

-Type III Construction (Semi-Rigid Framing)

$$M_u = M_w/\emptyset.6 \qquad (5.1)$$

resulting in a factor of safety of 1.67.

-Type I Construction (Rigid or Continuous Framing)

$$M_u = M_w/(\emptyset.6 \times \emptyset.8\emptyset) = M_w/\emptyset.48 \qquad (5.2)$$

where the Ø.8 factor limits the connection rotation to 1Ø% of the simple span rotation at the factored (ultimate) load with a factor of safety of 1.67.

The required bolt size can then be determined using Equations 3.4 to 3.16 and

$$d_b = \sqrt{2B_1/(\pi x F_a)} \qquad (5.3)$$

where F_a = the allowable stress of the bolt material. In

the AISC Specification [14], the allowable tensile stress for A325 bolt material is 44 ksi with a factor of safety against yielding of 2.Ø. Equation 5.3 reflects this factor of safety. The recommended procedures are demonstrated in the following design examples.

Design Example (1) Determine the required end-plate thickness and bolt size for a one-row, two-bolt flush end-plate for a built up beam with dimensions below and a working moment of 55 ft-kips, A572 Gr. 5Ø steel, A325 bolts, and Type III Construction.

$h = 16$ in. $\quad b_f = 6$ in. $\quad p_f = 1.5$ in. $\quad L = 24$ ft.
$t_w = .25$ in. $\quad t_f = .25$ in. $\quad g = 3$ in.

Step 1. Determine M_u and required end-plate thickness.

$$M_u = 55/Ø.6 = 91.67 \text{ ft-kips}$$

$$s = 1/2\sqrt{6x3} = 2.12 \text{ in.}$$

$$p_t = 1.5 + Ø.25 = 1.75$$

$$t_p = \left\{ \frac{91.67x12/5Ø}{[6/2(1/1.5+1/2.12) + (2.12+1.5)2/3](16-1.75)} \right\}^{1/2}$$

$$= Ø.515 \text{ in.} \qquad \underline{\text{Try PL 6x5/8}}$$

Step 2. Compute the flange force, F_f.

$$F_f = (91.67x12)/(16-Ø.25) = 69.84 \text{ kips}$$

Step 3. Find the thick plate limit, t_1.

$$t_1 = \sqrt{4.21(1.5)69.84/(6x50)}$$

$$= 1.212 \text{ in.} >> t_p = 0.625 \text{ in.}$$

Therefore, $Q \neq 0$

Step 4. Determine the thin plate limit, t_{11}.

Assume $d_b = 7/8$ in.

$w' = 6/2 - (7/8 + 1/16) = 2.06$ in.

$F_{yb} = 88$ ksi for A325 material

Approximate thickness

$$t_{11} = \sqrt{\frac{2(69.84x1.5 - \pi (.875)^3(88)/16)}{50(0.85x6/2 + 0.8x2.06)}}$$

$$= 0.942 \text{ in.}$$

Check the shear limitation.

$F_f < 2(2.06)(0.942)(50)/\sqrt{3} = 112.0$ kips
$69.64 < 112.0$ OK

Using the exact equation

$$t_{11} = \sqrt{\frac{2(69.84 \text{ x } 1.5 - \pi (.875)^3 88/16)}{6/2\sqrt{50^2 - 3\left(\frac{69.84}{.942 \text{ x } 6}\right)^2} + 2.06\sqrt{50^2 - 3\left(\frac{69.84}{2(2.06).942}\right)^2}}}$$

$$= 0.928 \text{ in.} \approx 0.942 \text{ in.}$$

Since $t_{11} > t_p = .625$ in. $Q=Q_{max}$

Step 5. Determine prying force, Q

$$F_{limit} = \frac{.625^2 x 50(0.85x6/2 + 0.8x2.06) + \pi(.875)^3 \, 88/8}{4x1.5}$$

$= 17.52$ kips

$(F_f)_{max}/2 = 6x.25x50/2 = 37.5$ kips

Thus, F' = 17.52 kips

$a = 3.682(.625/.875)^3 - .085 = 1.257$ in.

$$Q = \frac{2.06(.625)^2}{4x1.257} \sqrt{50^2 - 3\left(\frac{17.52}{2.06x.625}\right)^2}$$

$= 7.06$ kips

Step 6. Select bolt diameter

$B = 69.84/2 + 7.06 = 41.98$ kips

$d_b = \sqrt{2x41.98/(\pi x44)} = 0.779$ in. < 0.875 in.

Use PL 6x5/8 A572 Gr 50 with 2-7/8 in. diameter A325 bolts
The resulting connection strength is 135.2 ft-kips.

Using the same procedure for Type I Construction, M_u = 55/0.48 = 114.6 ft-kips, the required plate thickness is 0.576 in. and required bolt diameter is 0.857 in., resulting in the same requirements as used for the Type III design.

Design Example (2) For the working moment and geometry given in Example (1), determine the required end-plate thickness and bolt size for a four-bolt, flush unstiffened end-plate, p_b=3.Ø and Type III Construction.

Step 1. Determine M_u and required end-plate thickness.

$$M_u = 55/Ø.6 = 91.67 \text{ ft-kips}$$

$$u = 1/2\sqrt{6x3.Øx(16-3-1.75)/(16-1.75)} = 1.88 \text{ in.}$$

$$t_p = \left\{ \frac{91.67x12/5Ø}{(16-1.75)[6/2(1/1.5+1/1.88)+2/3(1.5+3+1.88)]-6(3)/(2x1.88)} \right\}^{1/2}$$

$$= Ø.453 \text{ in.} \qquad \underline{\text{Try PL 6 x 1/2}}$$

Step 2. Compute the flange force, F_f.

$$F_f = 91.67x12 \;/\; (16 - Ø.25) = 69.84 \text{ kips}$$

Step 3. Find the thick plate limit, t_l.

same as Example (1), $t_l = 1.212 >> t_p = Ø.5$ in.
Therefore, $Q \neq Ø$

Step 4. Determine the thin plate limit, t_{ll}.

Assume d_b = 3/4 in.

$$w' = 6/2 - (3/4 + 1/16) = 2.19 \text{ in.}$$

Approximate thickness

$$t_{ll} = \sqrt{\frac{2(69.84x1.5 - \pi(.75)^3 88/16)}{5Ø(Ø.85x6/2 + Ø.8x2.19)}}$$

$= 0.952$ in.

Check shear limitation

$F_f < 2(2.19)(.952)50 / \sqrt{3} = 120.4$ kips.
$69.84 < 120.4$ OK

Using the exact equation

$$t_{11} = \sqrt{\frac{2(69.84 \times 1.5 - \pi(.75)^3 88/16}{6/2\sqrt{50^2 - 3\left(\frac{69.84}{.952 \times 6}\right)^2} + 2.19\sqrt{50^2 - 3\left(\frac{69.84}{2 \times 2.19 \times .952}\right)^2}}}$$

$= 0.931$ in. $\simeq 0.952$ in.

Since $t_{11} > t_p = 0.5$ in., $Q = Q_{max}$

Step 5. Determine the prying force, Q.

$$F_{limit} = \frac{.5^2 \times 50(.85 \times 3 + .8 \times 2.19) + \pi(.75)^3 88/8}{4 \times 1.5}$$

$= 11.39$ kips $< (F_f)_{max}/2$

Thus, $F' = 11.39$ kips

$a = 3.682(.5/.75)^3 - 0.085 = 1.01$

$$Q_{max} = \frac{(2.19).5^2}{4 \times 1.01}\sqrt{50^2 - 3\left(\frac{11.39}{2.19 \times .5}\right)^2}$$

$= 6.32$ kips

Step 6. Select bolt diameter, d_b

$B_1 = 3(69.84)/8 + 6.32 = 32.51$ kips

$B_2 = F_f/8 = 69.84/8 = 8.73$ kips

Select all bolts for B_1.

$$d_b = \sqrt{2x32.51/(\pi x44)}$$

$= 0.686$ in. < 0.75 in. OK

Use PL 6x1/2 A572 Gr 50 with 4-3/4 in. diameter A325 bolts. The resulting connection strength is 111.5 ft-kips.

Using the same procedure for Type I Construction, M_u = 55/0.48 = 114.6 ft-kips, the required plate thickness is 0.507 in. and required bolt diameter is 0.736 in. Therefore, a PL 6x5/8 A572 gr 50, with 4-3/4 in. diameter A325 bolts is recommended, connection strength = 174.3 ft-kips.

Design Example (3) For the working moment and geometry given in Example (1), determine the required thickness and bolt size for a four-bolt stiffened flush end-plate with a gusset plate placed between the two rows of tension bolts. Assume Type III Construction with p_b=3.0 in. and t_s=0.375 in.

Step 1. Determine M_u and end-plate thickness.

$M_u = 55/0.6 = 91.67$ ft-kips

$s = 1/2\ \sqrt{6x3} = 2.12$ in.

$$p_s = 1/2(3-\emptyset.375) = 1.31 \text{ in.}$$

$$t_p = \left\{ \frac{91.67x12/5\emptyset}{(16-1.75)[6/2(1/1.5+1/1.31)+(1.5+1.31)2/3] + \frac{}{(16-1.75-3)[6/2(1/1.31+1/2.12)+(1.31+2.12)2/3]} \right\}^{1/2}$$

$= \emptyset.376$ in. Try PL 6 x 3/8

Step 2. Compute flange force, F_f

$$F_f = 91.67x12/(16-\emptyset.25) = 69.84$$

Step 3. Find the thick plate limit, t_1

same as Example (1), $t_1 = 1.212 >> t_p = \emptyset.375$ in

Therefore, $Q \neq \emptyset$.

Step 4. Determine the thin plate limit, t_{11}.

Assume $d_b = 3/4$ in.

Same as Example (2), $Q=Q_{max}$

Step 5. Determine prying force, Q

$$F_{1limit} = \frac{\emptyset.375^2x5\emptyset(\emptyset.85x3+\emptyset.8x2.19)+ \pi(.75)^3 88/8}{4x1.5}$$

$$= 7.47 \text{ kips} = F'$$

$$a = 3.682(\emptyset.375/\emptyset.75)^3 - \emptyset.\emptyset85 = \emptyset.375 \text{ in.}$$

$$Q_{max} = \frac{(2.19)(.375)^2}{4x\emptyset.375}\sqrt{50^2 - 3\left(\frac{7.47}{2.19x.375}\right)^2}$$

$$= 9.74 \text{ kips}$$

Step 6. Select bolt diameter, d_b

$$B_1 = 3(69.84)/10 + 9.74 = 30.69 \text{ kips}$$
$$B_2 = F_f/5 = 69.84/5 = 13.97 \text{ kips}$$

Select all bolts for B_1.

$$d_b = \sqrt{2x30.69/(\pi x44)} = \emptyset.666 \text{ in.} < \emptyset.75 \text{ in} \quad \text{OK}$$

Use PL 6x3/8 A572 Gr 50 with 4-3/4 in. diameter A325 bolts The resulting connection strength is 90.9 ft-kips.

Using the same procedure for Type I Construction, M_u = 114.6 ft-kips, the required plate thickness is Ø.421 in. and required bolt diameter is Ø.686 in. Therefore, a PL 6x1/2 A572 Gr 50 with 4-3/4 in. diameter A325 bolts is recommended, connection strength = 161.6 ft-kips.

<u>Design Example (4)</u> For the working moment and geometry given in Example (1), determine the thickness and bolt size for a four-bolt <u>stiffened</u> flush end-plate with a gusset plate placed outside the two rows of tension bolts. Assume Type III Construction with p_b=3.Ø in. and t_s=Ø.375 in.

Step 1. Determine M_u and end-plate thickness.

$$M_u = 55/\emptyset.6 = 91.67 \text{ ft-kips}$$

$$p_s = d_b + 1/2 = \emptyset.75 + \emptyset.5 = 1.25 \text{ in.}$$

$$h_t = h - p_t - p_b - p_s = 16 - 1.75 - 3 - 1.25 = 10 \text{ in.}$$

$$t_p = \left\{ \frac{91.67 \times 12/50}{(16-1.75)[6/(2\times1.5)+2/3(1.5+3)] + 6/4 + 1.25(16-1.5-3)} \right\}^{1/2}$$

$$= 0.410 \text{ in.} \qquad \underline{\text{Try PL 6 x 1/2}}$$

Step 2. Compute flange force, F_f

$$F_f = 91.67 \times 12/(16-0.25) = 69.84 \text{ kips}$$

Step 3. Find the thick plate limit, t_1

same as Example (1), $t_1 = 1.212 >> t_p = 0.5$ in.

Therefore, $Q \neq 0$

Step 4. Determine the thin plate limit, t_{11}

same as Example (2), Assume $d_b = 3/4$ in.

$Q = Q_{max}$

Step 5. Determine prying force, Q

F_{limit} same as Example (2) = 11.39 kips

$a = 1.01$ in. and $Q_{max} = 6.32$ kips from Example 2

Step 6. Select bolt diameter, d_b

$$B_1 = 3(69.84)/8 + 6.32 = 32.51 \text{ kips}$$

$$d_b = \sqrt{2x32.51/(\pi x44)} = 0.686 \text{ in.} < 0.75 \text{ in. OK}$$

Use PL 6x1/2 A572 Gr 50 with 4-3/4 in. diameter A325 bolts The resulting connection strength is 136.0 ft-kips.

Using the same procedure for Type I Construction, M_u = 55/0.48 = 114.6 ft-kips, the required plate thickness is 0.459 in. and required bolt diameter is 0.736 in., resulting in the same requirements as used for the Type III design.

From Table 5.1, for Type I Construction (Rigid or Continuous Framing) with a working moment of 55 ft-kips, and a span length of 24 ft., 3/4 in. diameter bolts and a 1/2 in. thick end-plate are required for both stiffened, four-bolt flush end-plate connections; 3/4 in. bolts and a 5/8 in. thick end-plate are required for the unstiffened, four-bolt flush end-plate connection; and 7/8 in. bolts and a 5/8 in. thick end-plate are required for the two-bolt flush end-plate configuration. The actual connection strength for the stiffened end-plate connection is 20% stronger if the stiffener is <u>between</u> the tension rows of bolts rather than <u>outside</u>. The connection strength of the four-bolt, unstiffened end-plate connection is 30% stronger than that of the two-bolt connection and requires a smaller bolt as well.

For Type III Construction (Semi-Rigid Framing), 3/4 in. diameter bolts are required for both the stiffened and unstiffened four-bolt connections while 7/8 in. diameter bolts are required for the two-bolt connection. For stiffened <u>outside</u> and unstiffened four-bolt connections, a 1/2 in. thick end-plate is required, while a 5/8 in. thick end-plate is needed with the two-bolt connection. The

Table 5.1

Summary of Flush End-Plate Design Examples

		Construction Type	Bolt Diameter (in.)	Required Plate Thickness (in.)	Connection Strength (ft-kips)
	Two-Bolt	I	7/8	5/8	135.2
		III	7/8	5/8	135.2
	Four-Bolt	I	3/4	5/8	174.3
		III	3/4	1/2	111.5
	Between	I	3/4	1/2	161.6
		III	3/4	3/8	90.9
	Outside	I	3/4	1/2	136.0
		III	3/4	1/2	136.0

Notes: M_w = 55 ft-kips and L = 24 ft.

required end-plate thickness can be reduced to 3/8 in. if a stiffener is placed between the tension rows of bolts. The connection strength of the four-bolt stiffened outside connection is 22% stronger than the four-bolt unstiffened connection.

CHAPTER VI

SUMMARY AND FINDINGS

6.1 Summary

The unification of design procedures for four types of flush end-plate configurations: two-bolt unstiffened; four-bolt unstiffened; four-bolt stiffened with a web gusset plate between the tension rows of bolts; and four-bolt stiffened with a web gusset plate outside the tension rows of bolts has been described in the preceding chapters. The unification attempt resulted in consistent yield-line based design equations for the four types of end-plate configurations and uniform procedures to estimate bolt forces considering prying action. Verification of the analytical models was done with experimental testing. Comparisons among configurations was also presented based on strength, from required end-plate thickness and resulting moment capacity, and stiffness, from moment-rotation (M-O) curves and rigid connection limiting moment ratios.

6.2 Findings

The yield-line mechanisms presented in Chapter II (Figures 2.1 through 2.4) and resulting ultimate moment capacity equations (Equations 2.11, 2.13, 2.15, and 2.17),

adequately predict strength for the four flush end-plate configurations examined. The ratio of the applied to predicted moment for the two-bolt, unstiffened flush end-plate configuration varied from Ø.94 to 1.Ø8 and for the four-bolt, unstiffened flush end-plate configuration from Ø.97 to 1.Ø6. The same ratio for the four-bolt, stiffened, flush end-plate configurations varied from Ø.92 to 1.Ø6 and Ø.98 to 1.Ø8 for the stiffened between and stiffened outside configurations, respectively. For all four flush end-plate configurations, the average applied to predicted moment ratio was 1.Ø2 with a standard deviation of ±Ø.Ø5. From Table 2.9, the stiffened between configuration is approximately 9Ø% stronger than the two-bolt, unstiffened configuration, 5Ø% stronger than the four-bolt unstiffened configuration and 25% stronger than the four-bolt stiffened outside configuration. The stiffened outside configuration is approximately 6Ø% stronger than the two-bolt unstiffened configuration and 2Ø% stronger than the four-bolt unstiffened configuration. Finally, the four-bolt unstiffened configuration is approximately 3Ø% stronger than the two-bolt unstiffened configuration.

The modified Kennedy et. al. procedure was shown to adequately predict bolt forces to the proof load for all four end-plate configurations. For the two-bolt unstiffened configuration, the predicted bolt forces were slightly unconservative (1Ø% to 15%), while for the four-bolt, stiffened and unstiffened configurations very good correlation (within 5%) was found. The ratio of the moment at proof load to the failure moment of the connection (Table 3.1) was found to vary from Ø.62 to 1.ØØ for the two-bolt unstiffened cases, Ø.63 to 1.Ø5 for the four-bolt unstiffened cases, Ø.71 to 1.Ø9 for the four-bolt stiffened between cases, and Ø.78 to 1.1Ø for the four-bolt

stiffened outside cases. The average ratio for all tests was Ø.86 with a standard deviation of ± Ø.16.

The ratio of the "thick" plate moment predicted by the modified Kennedy method to the failure moment ranged from Ø.47 to Ø.85 (Table 3.1) with an average of Ø.64 and a standard deviation of 12% for all end-plate configurations.

Chapter IV presented moment-rotation curves with corresponding beam lines for the four end-plate configurations. The beam-lines shown in Figure 4.4 and Appendix C are based on the actual length of the test setup. If variations in the length are made then a similar variation occurs in the beam-line. The average limiting moment using the testing span lengths for a rigid framing (Type I Construction) connection was found to be approximately 83% of the failure moment for all four configurations with a standard deviation of ±Ø.12. From Figure 4.6, a four-bolt stiffened or unstiffened flush end-plate is shown to be 1Ø-14% stiffer than a two-bolt, flush end-plate. The stiffness among four-bolt flush end-plate configurations was found to be relatively the same.

Finally, design procedures are presented in Chapter V but are limited to the geometric parameters defined in Chapter II. The design procedures are in an allowable stress design format with implied a factor of safety of 1.67 against end-plate failure and 2.Ø against bolt yielding. The design moments for rigid framing connections (Type I Construction) must be limited to a value less than the full strength of the connection to insure sufficient stiffness. The connection curve/beam-line concept was found to be useful in determining this limiting moment. A study of the final design equations shows that the ideal

geometry uses minimum bolt pitch, p_f and bolt gage, g. Further, for four-bolt connections, the pitch between bolts, p_b, should be between the allowed minimum p_b and approximately four bolt diameters.

REFERENCES

1. Srouji, R., Murray, T., and A. Kukreti, "Yield-Line Analysis of End-Plate Connections with Bolt Force Predictions", Fears Structural Engineering Laboratory Report No. FSEL/MBMA 83-05, University of Oklahoma, Norman, Oklahoma, December 1983.

2. Douty, R.T. and W. McGuire, "High Strength Bolted Moment Connections", Journal of the Structural Division, ASCE, Vol. 91, No. ST2, April, 1965, pp. 101-128.

3. Bockley, D.I., "The Design of Single Story Pitched Roof Portal Frames", BCSA Brochure, 1970.

4. DSTV/DAST, Moment and Plate Connections with HSFG Bolts (in German), IHE 1, 1978.

5. Norme Francaise Enregistree, Metal Construction, Jointing by Means of Bolts Controlled Tightening, Structural Requirements and Checking of Jointing (in French), NF, 1979, pp. 22-460.

6. Zoetemeijer, P., "A Design Method for the Tension Side of Statically Loaded, Bolted Beam-to-Column Connections", Heron, Vol. 20, No. 1, The Netherlands, 1974, pp. 1-59.

7. Packer, J.A., amd L.J. Morris, "Behavior and Design of Haunched Steel Portal Frame Knees", Research Report M002, Simon Engineering Laboratories, University of Manchester, England, 1975.

8. Phillips, J. and J.A. Packer, "The Effect of Plate Thickness on Flush End-Plate Connections", Joints in Structural Steelwork, Proceedings of the International Conference on Joints in Steelwork, held at Middlesbrough, Clevelend, United Kingdom Pentech Press, London, England, 1981, pp. 6.77-6.92.

9. Kennedy, N.A., Vinnakota, S., and A.N. Sherbourne, "The Split-Tee Analogy in Bolted Splices and Beam-Column Connections", Joints in Structural Steelwork, Proceedings of the International Conference on Joints in Steelwork, held at Middlesbrough, Cleveland, John Wiley and Sons, New York - Toronto, 1981, pp. 2.138-2.157.

10. Hendrick, D., Murray, T., and A. Kukreti, "Analytical and Experimental Investigation of Stiffened Flush End-Plate Connections with Four-Bolts at the Tension Flange", Fears Structural Engineering Laboratory Report No. FSEL/MBMA 84-02, University of Oklahoma, Norman, Oklahoma, September 1984.

11. Mann, A.P. and L.J. Morris, "Limit Design of Extended End-Plate Connections", Journal of the Structural Division, ASCE, Vol. 105, No. ST3, March 1979, pp. 511-526.

12. Nair, R.S., Birkemoe, P.C. and W.H. Munse, "High Strength Bolts Subject to Tension and Prying", Journal of the Structural Division, ASCE, Vol. 100, No. ST2, February, 1974.

13. Manual of Steel Construction, 8th ed., American Institute of Steel Construction, Chicago, Illinois, 1980.

14. "Specification for the Design, Fabrication and Erection of Structural Steel for Buildings", American Institute of Steel Construction, New York, 1978.

APPENDIX A

NOMENCLATURE

NOMENCLATURE

a = distance to location of prying action

B = bolt force

B_1 = outer bolt force

B_2 = inner bolt force

b_f = beam flange width

c = $(b_f-g)/2$ = end-plate bolt edge distance

d_b = bolt diameter

ds = elemental length of line n

ds_x = the x-component of the elemental length ds

ds_y = the y-component of the elemental length ds

E = Young's modulas of elasticity

F = flange force per bolt

F_a = allowable bolt stress

f_b = bending stress

F_{by} = yield stress of beam material

F_f = flange force = $M_u/(d-t_f)$

F_{limit} = flange force at which the end-plate becomes "thin"

F_{py} = yield stress of plate material

F_{yb} = yield stress of beam material

g = gage distance between bolts

h = beam depth

h_t = distance between inner edge of stiffener and outer compression flange

L = length of beam

L_n = length of yield line n

M_u = ultimate moment at end-plate

M_{yb} = moment at which the experimental bolt force is at the

proof load (twice the allowable)

m_p = plastic moment capacity of plate per unit length, equal to $(F_{py}t_p^2)/4$

m_{px}, m_{py} = the x(y)-component of the normal moment capacity per unit length

N = number of yield lines in a mechanism

p_b = pitch between upper and lower rows of the tension bolts

p_f = pitch measured from bottom of flange to centerline of first bolt row

p_t = pitch measured from top of flange to centerline of the first bolt row

Q = prying force

s = distance from bolt centerline to the lower yield-line

t_f = flange thickness

t_p = end-plate thickness

t_s = stiffener thickness

t_l = thick plate limit

t_{ll} = thin plate limit

w_i = total internal energy stored

w = width of end-plate per bolt pair

w_{in} = internal work done in the nth yield-line

w' = width of end-plate per bolt at bolt line minus bolt hole diameter

Z = plastic section modulas

θ_n = relative normal rotation of yield-line n

θ_{nx} = the x-component of the relative normal rotation of the yield-line n

θ_{ny} = the y-component of the relative normal rotation of the yield-line n

θ = rotation of connection

APPENDIX B

BOLT FORCE VERSUS MOMENT PLOTS

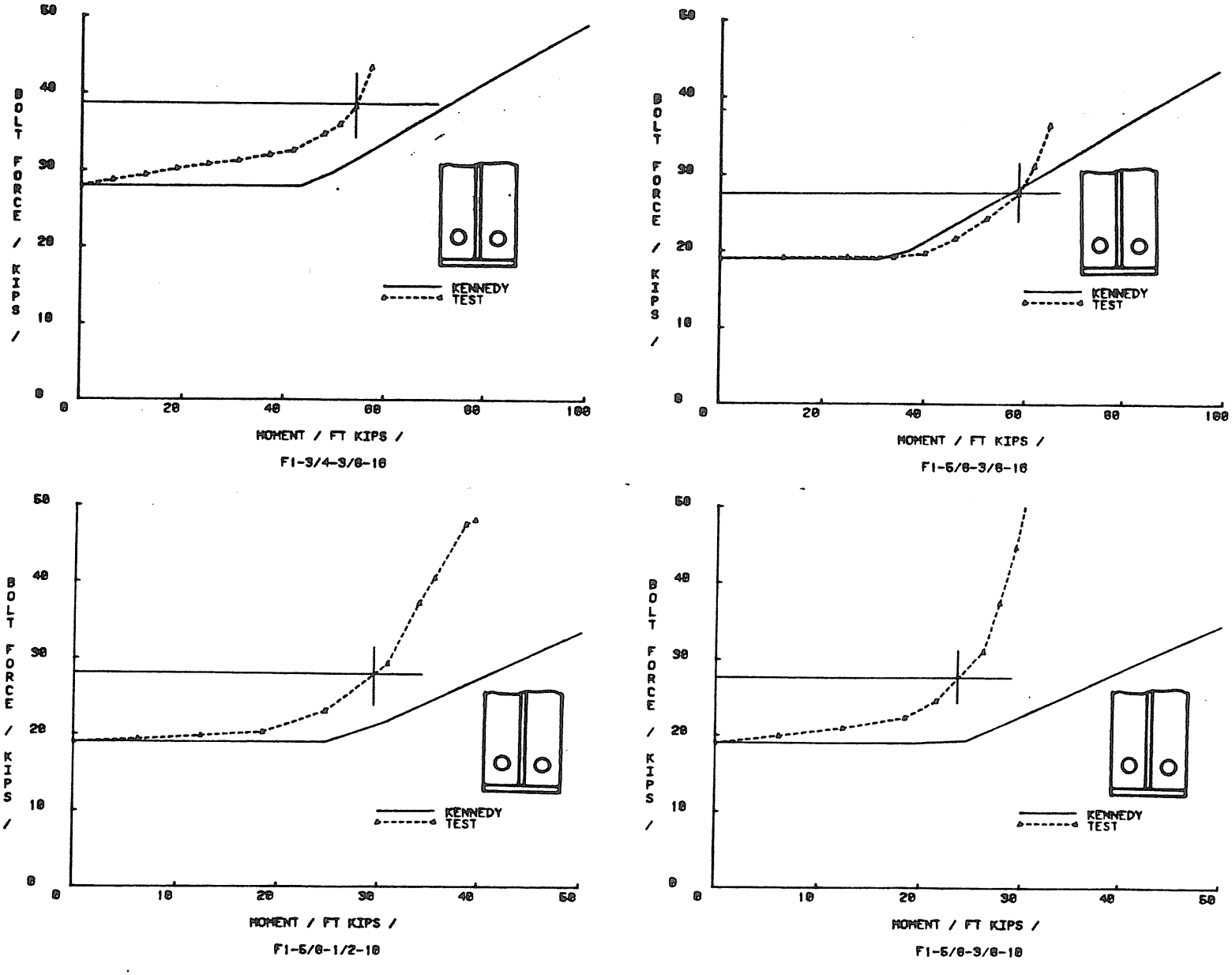

Figure B.1 Typical Bolt Force Versus Moment Relationship

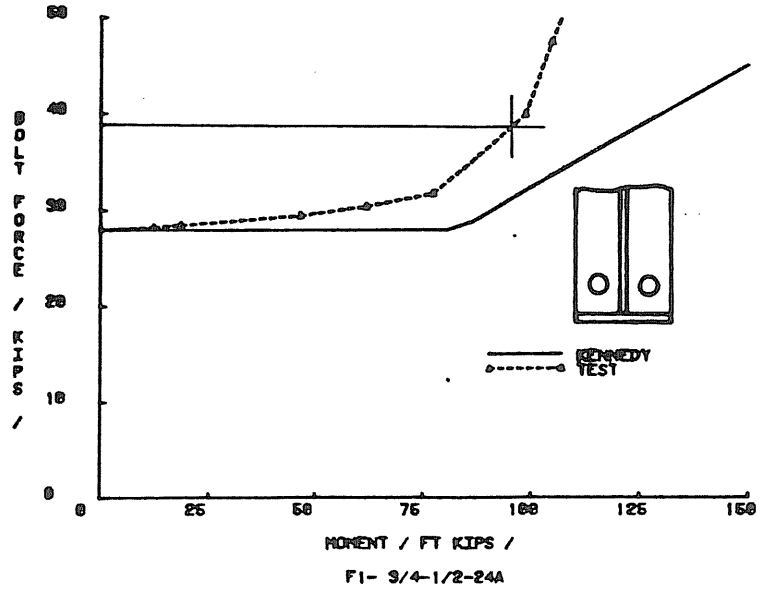

F1- 3/4-1/2-24A

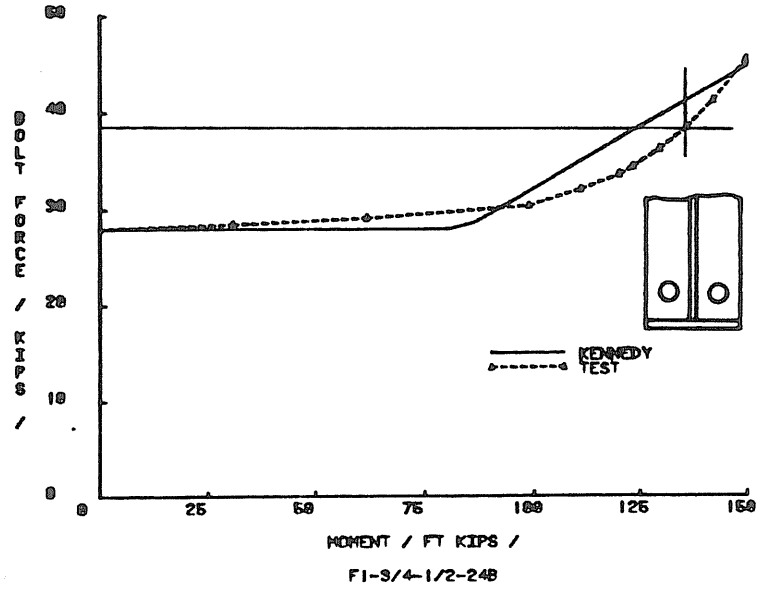

F1-3/4-1/2-24B

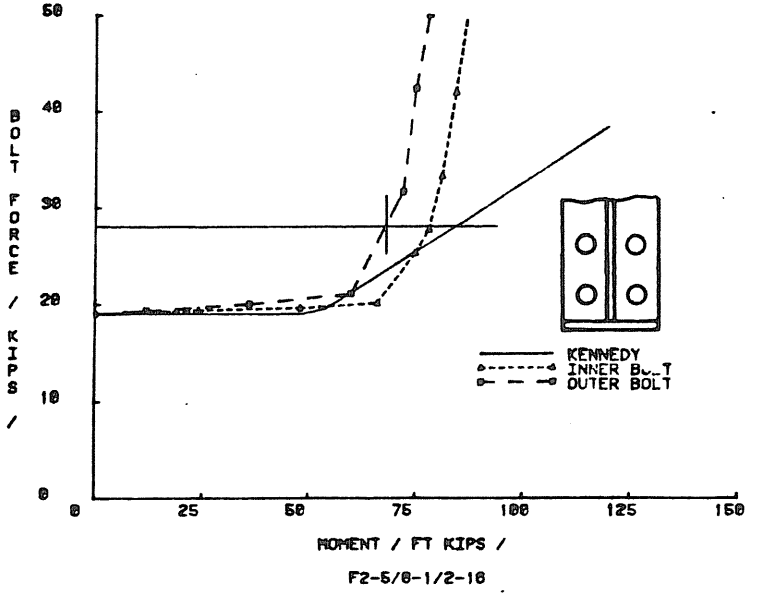

F2-5/8-1/2-16

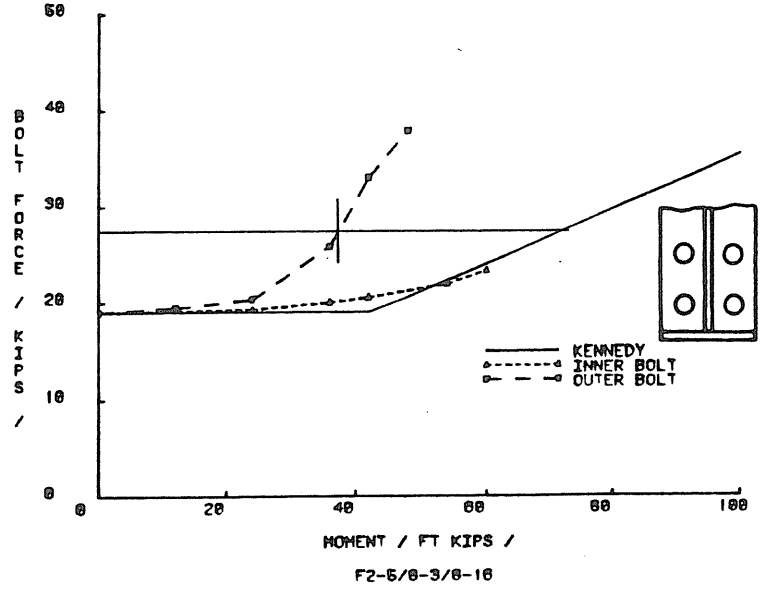

F2-5/8-3/8-16

Figure B.2 Typical Bolt Force Versus Moment Relationship

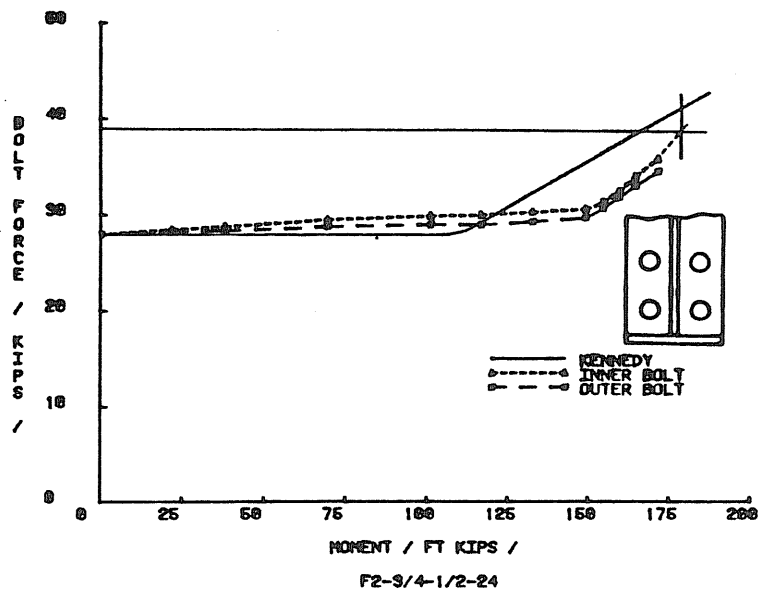

F2-3/4-1/2-24

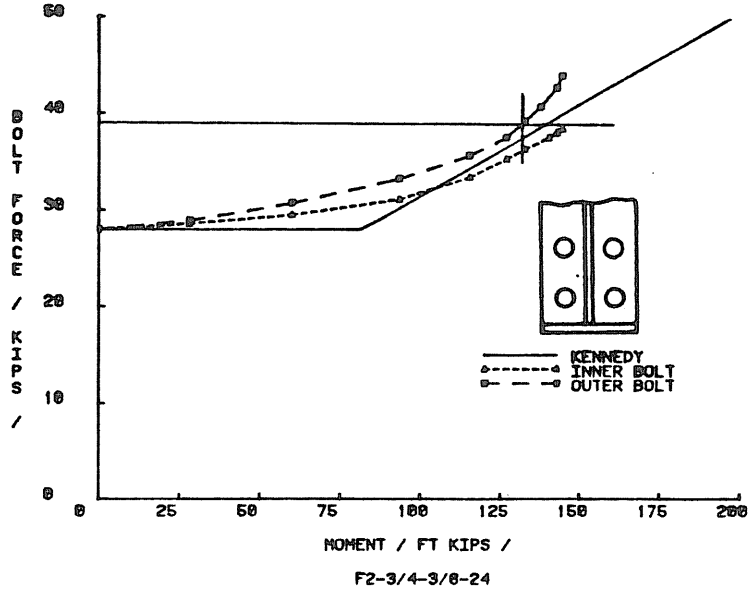

F2-3/4-3/8-24

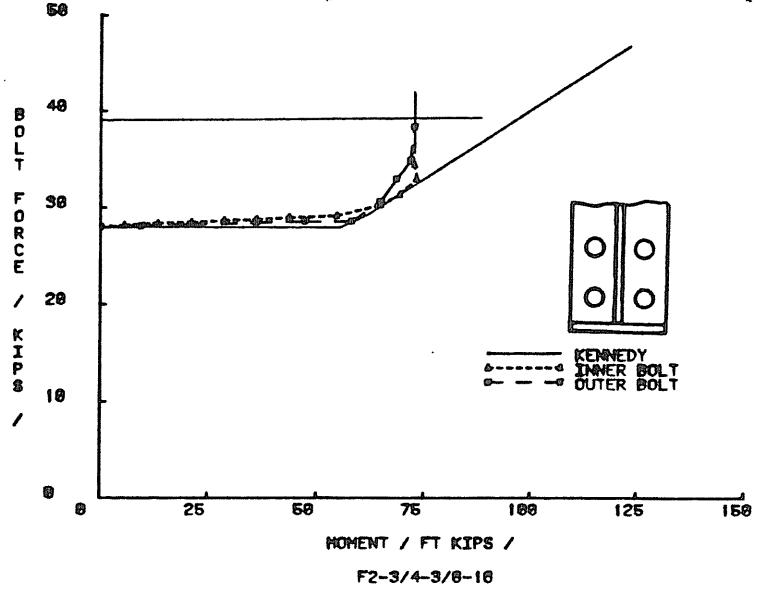

F2-3/4-3/8-16

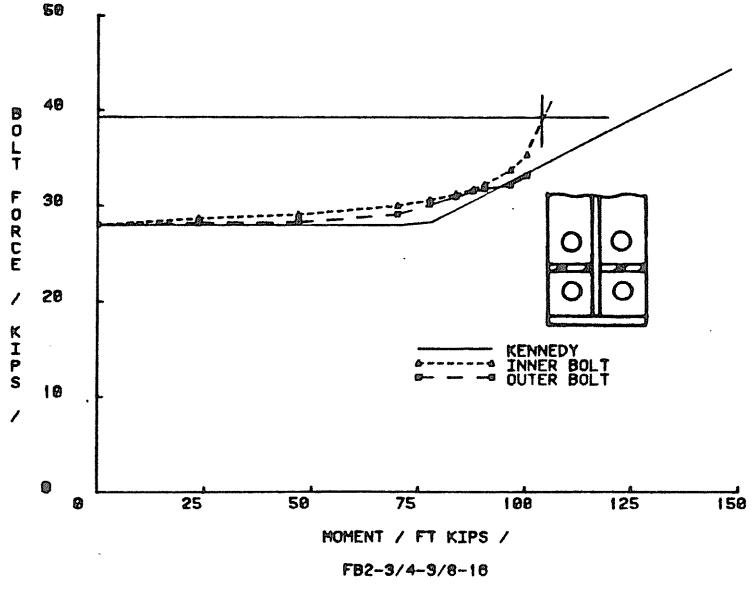

FB2-3/4-3/8-16

Figure B.3 Typical Bolt Force Versus Moment Relationship

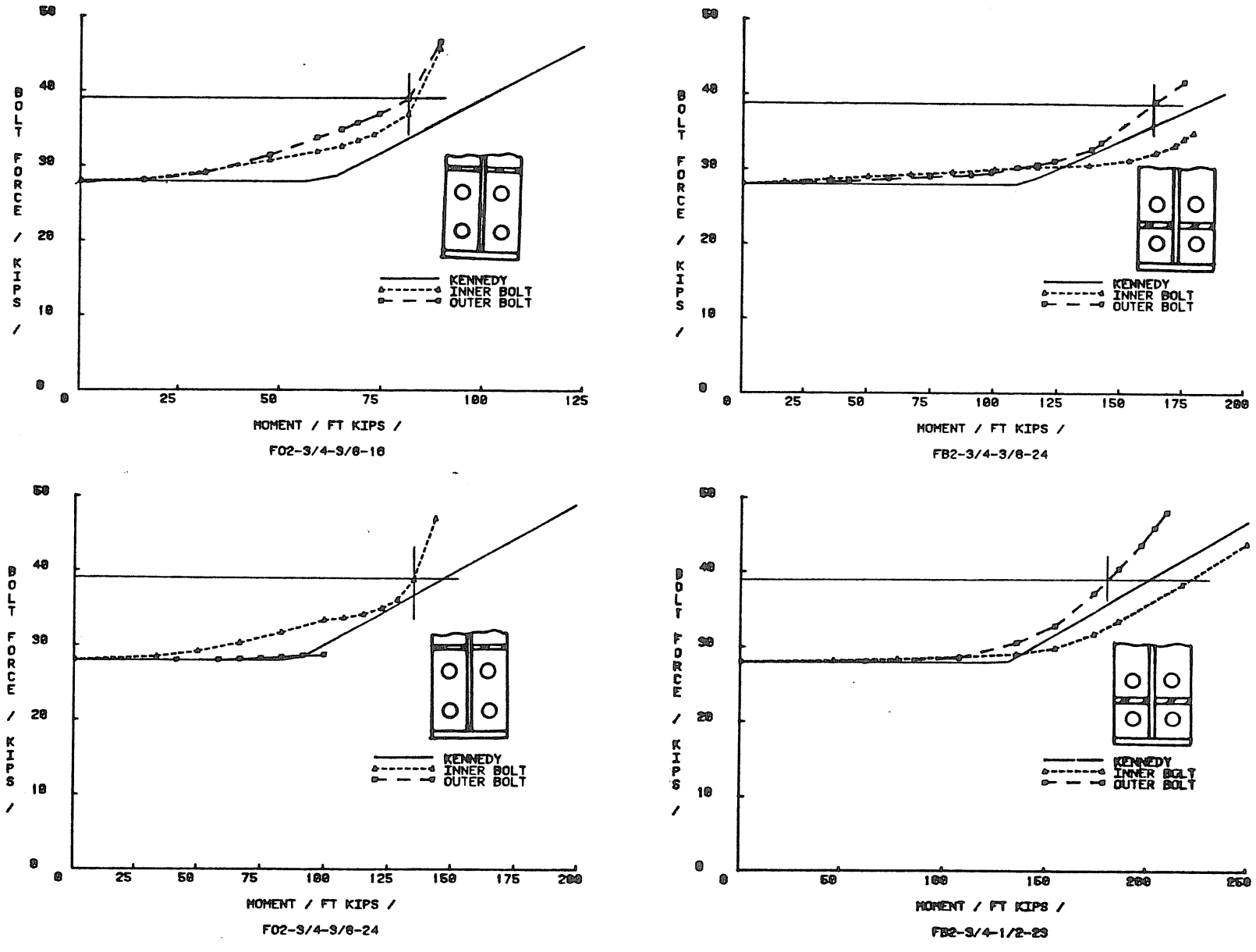

Figure B.4 Typical Bolt Force Versus Moment Relationship

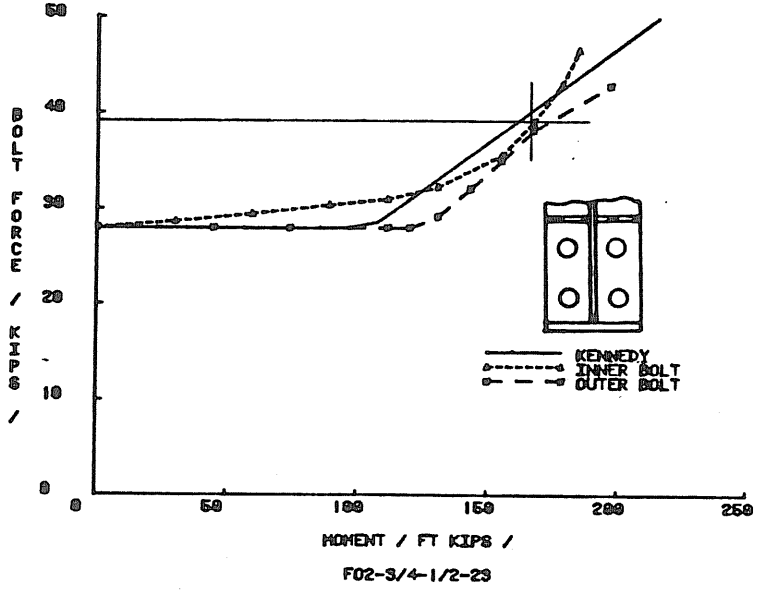

Figure B.5 Typical Bolt Force Versus Moment Relationship

APPENDIX C

MOMENT VERSUS ROTATION PLOTS

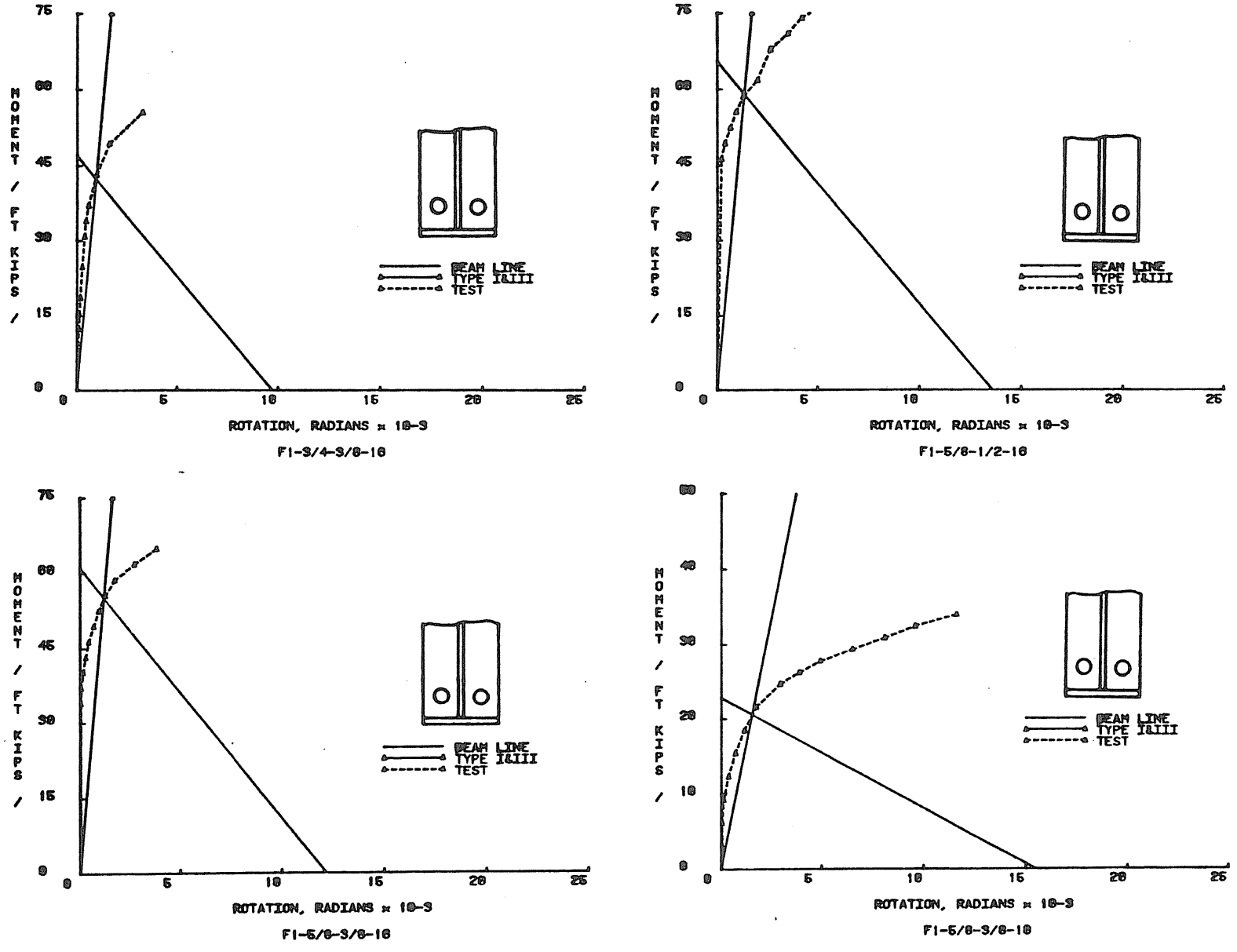

Figure C.1 Typical Moment Versus Rotation Relationship

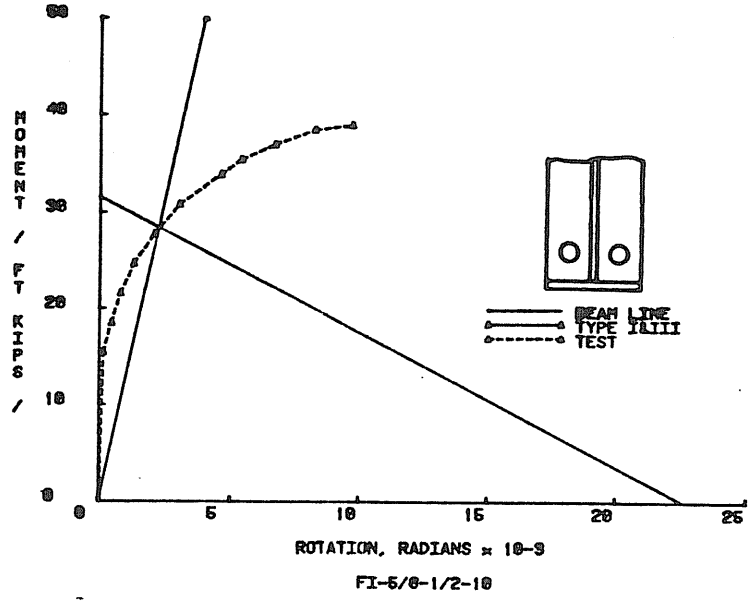

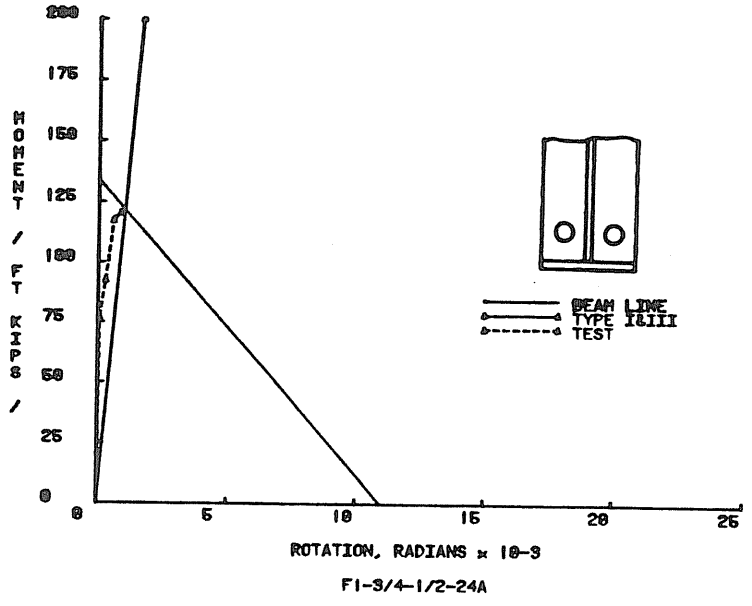

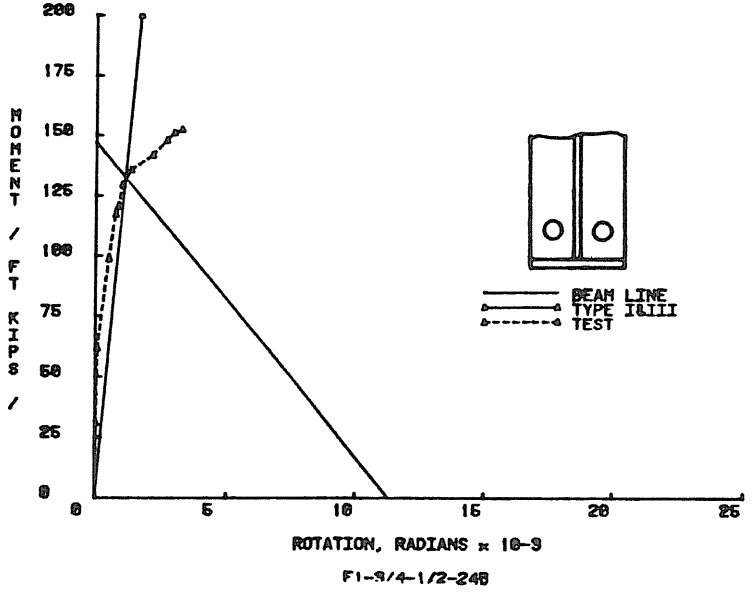

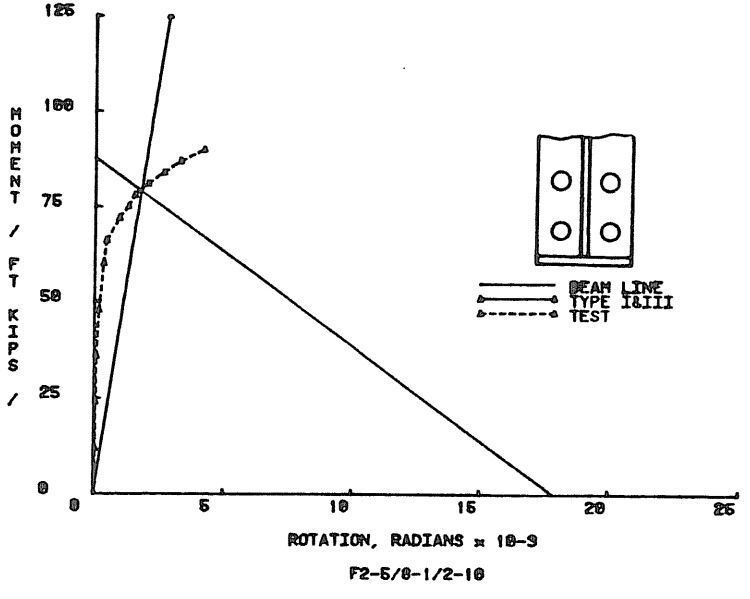

Figure C.2 Typical Moment Versus Rotation Relationship

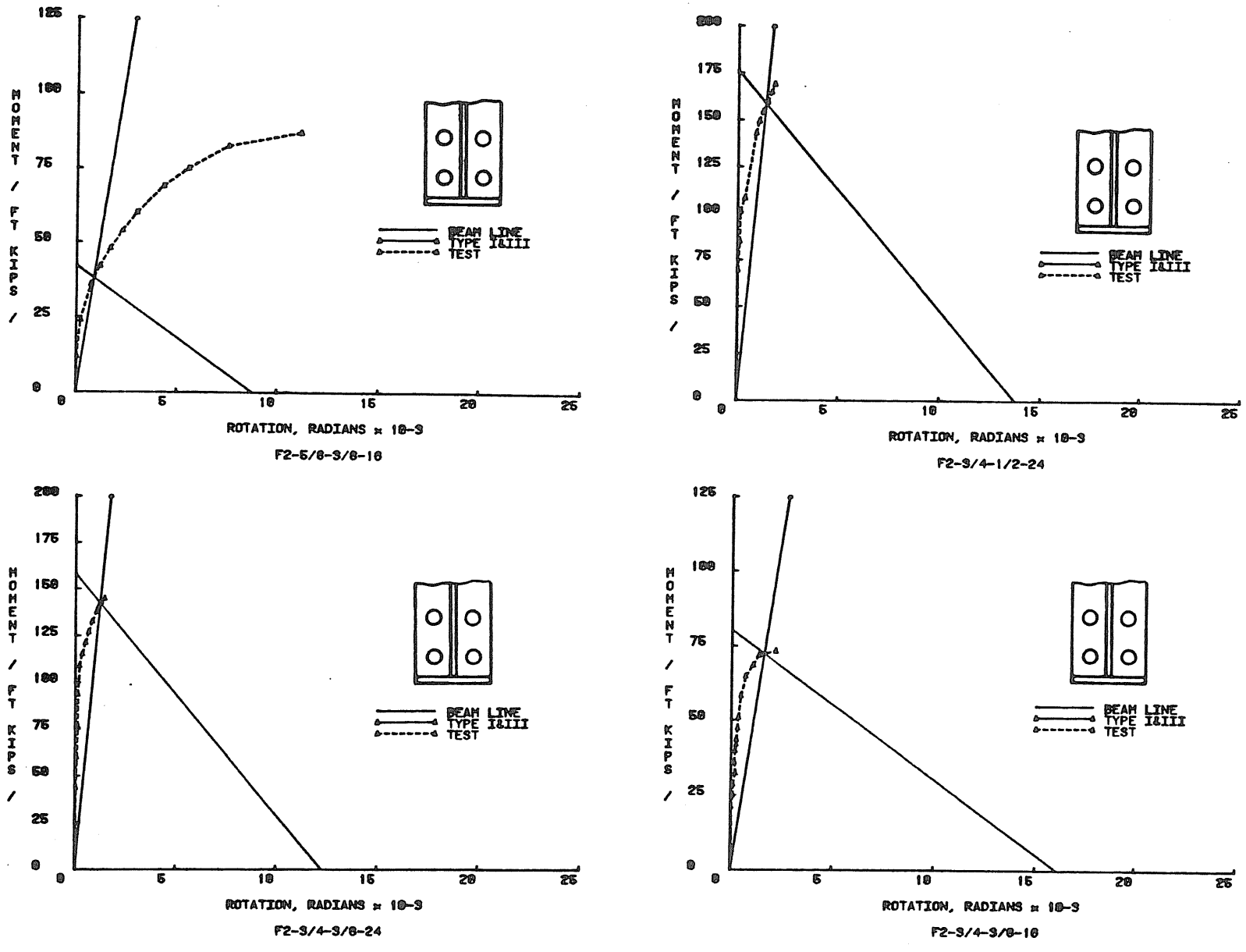

Figure C.3 Typical Moment Versus Rotation Relationship

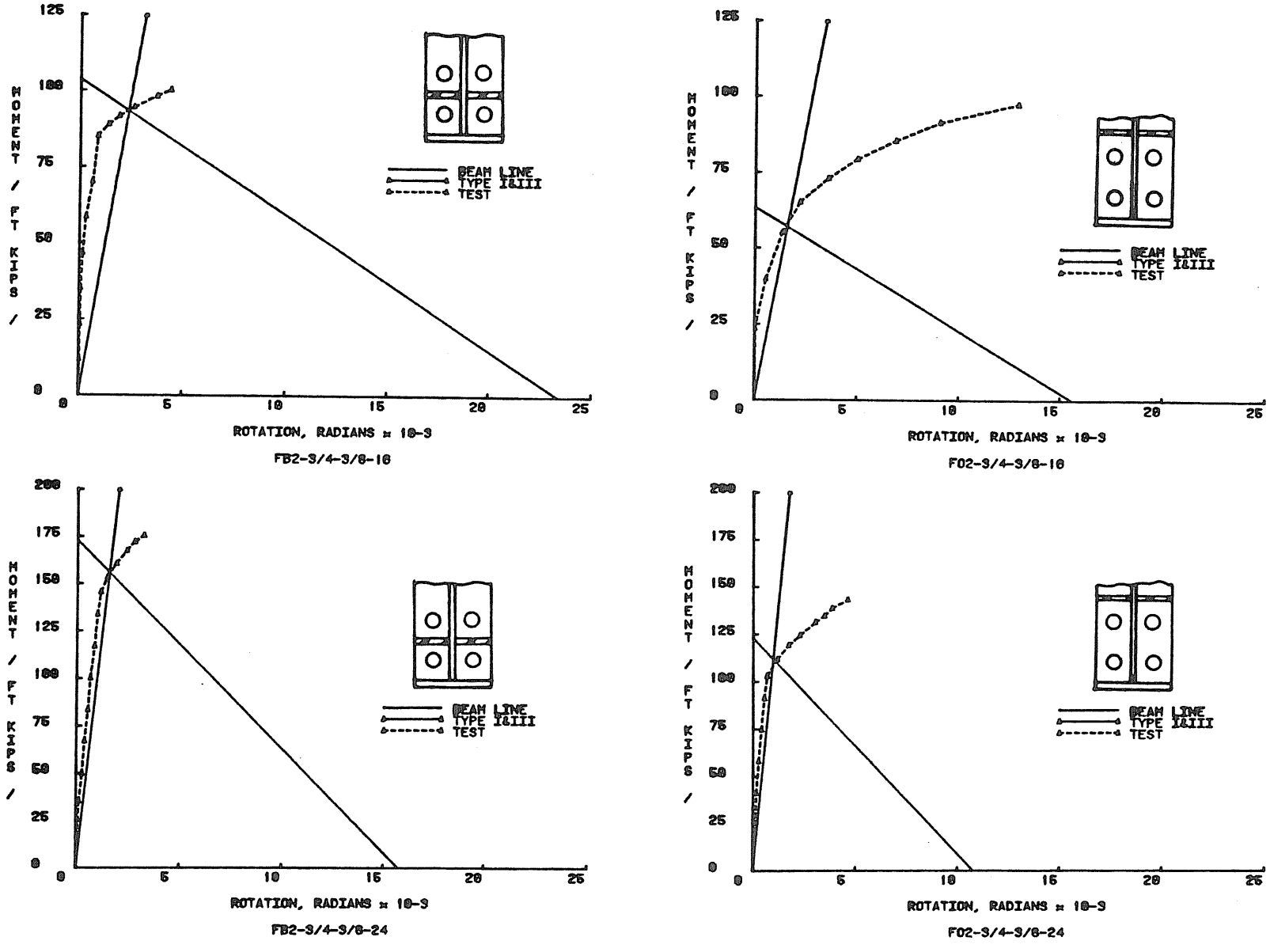

Figure C.4 Typical Moment Versus Rotation Relationship

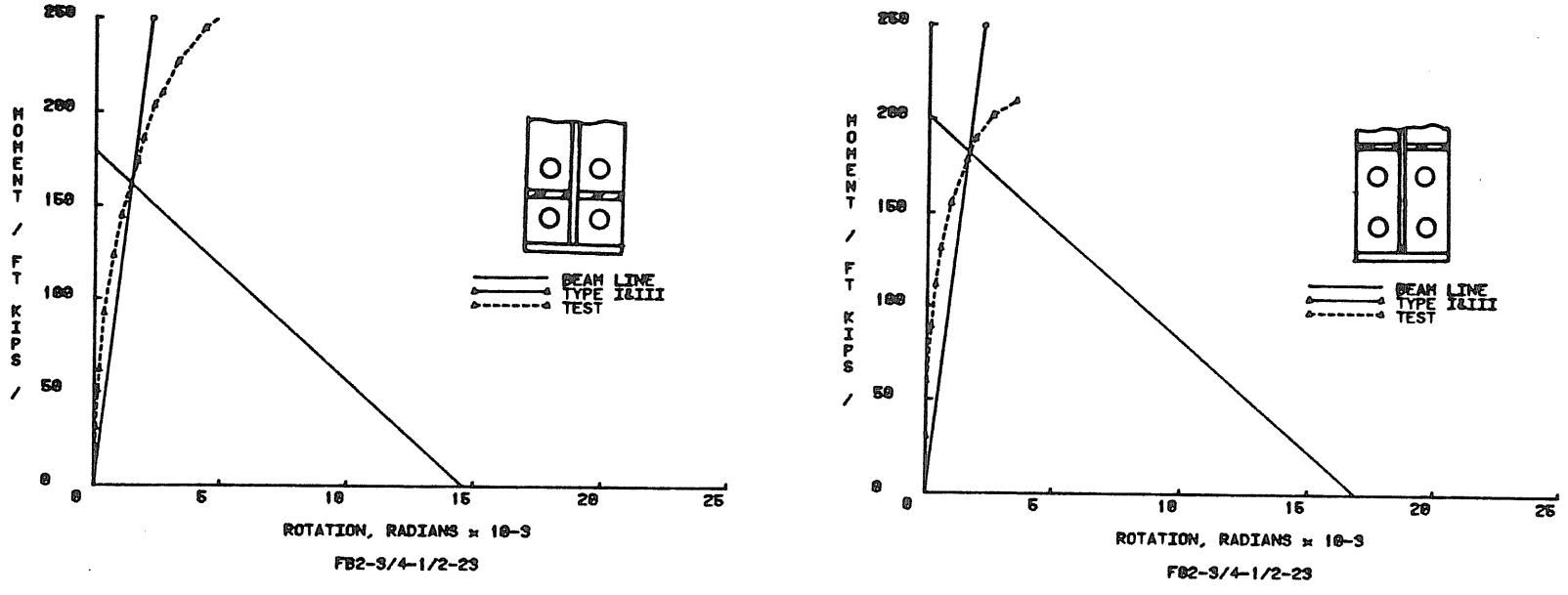

Figure C.5 Typical Moment Versus Rotation Relationship